Online Appendix D
Composite Likelihood for Stochastic Migration Model with Unobserved Factor *

Djogbenou, A.[1], Gouriéroux, C.[2], Jasiak J.[1], and M. Bandehali[3]

[1]York University
[2]Toronto University, Toulouse School of Economics and CREST
[3]Equitable (EQ) Bank, Toronto

March 15, 2023

Abstract

This online Appendix D examines the performance of the conditional Maximum Composite Likelihood (MCL) estimators for the stochastic factor ordered Probit model of credit rating transitions of firms. The conditional MCL estimators CL(1) and CL(2) are considered. Their performance at finite T is illustrated and compared with a granularity-based estimators in a simulation study.

*The authors gratefully acknowledge financial support of the chair of the Authority of Prudential Control and Resolution (ACPR)/Risk Foundation: Regulation and Systemic Risks, the ECR DYSMOIA and the Natural Sciences and Engineering Council of Canada (NSERC). We thank the anonymous referee for helpful comments.

Appendix D: Simulation Details and Additional Results

This online Appendix provides simulation results illustrating the finite sample properties of the MCL estimators of the stochastic migration model with an unobserved factor. Sections D.1 and D.2 illustrate the performance of the CL(1), CL(2) estimators of parameters $\hat{c}_k + 1,\ k = 2, ..., 7$ and $\hat{\beta}_j, \hat{\delta}_j, \hat{\sigma}_j\ j = 2, ..., 7$. For comparison, the finite sample properties of the granularity estimators of these parameters are examined in section D.3. Section D.4 shows the dynamics of simulated rating structure. The design of the experiment and the true parameter values are described in Section 5.1 of the main paper. We consider n=1000 firms and samples of size T=60, 120 and 240. The latent factor is assumed to follow an AR(1) model with coefficient ρ =0.0, 0.4, 0.7 and 0.95. The simulation results show that the CL(1) and CL(2) estimators are reliable in finite sample and their properties depend on size T and factor persistence ρ.

The composite log-likelihood at lag 2 involves an integral which cannot be computed analytically. This integral is the expected value of:

$$\sum_{l=1}^{K} \left[\Phi\left(\frac{c_{k+1} - \delta_l - \beta_l \rho f}{\sqrt{\sigma_l^2 + \beta_l^2(1-\rho^2)}} \right) - \Phi\left(\frac{c_k - \delta_l - \beta_l \rho f}{\sqrt{\sigma_l^2 + \beta_l^2(1-\rho^2)}} \right) \right] \times \left[\Phi\left(\frac{c_{l+1} - \delta_j - \beta_j f}{\sigma_j} \right) - \Phi\left(\frac{c_l - \delta_j - \beta_j f}{\sigma_j} \right) \right],$$

where the source of the randomness f follows a standard normal distribution. Therefore, it can be approximated by:

$$\frac{1}{S} \sum_{s=1}^{S} \sum_{l=1}^{K} \left[\left[\Phi\left(\frac{c_{k+1} - \delta_l - \beta_l \rho f_s}{\sqrt{\sigma_l^2 + \beta_l^2(1-\rho^2)}} \right) - \Phi\left(\frac{c_k - \delta_l - \beta_l \rho f_s}{\sqrt{\sigma_l^2 + \beta_l^2(1-\rho^2)}} \right) \right] \times \left[\Phi\left(\frac{c_{l+1} - \delta_j - \beta_j f_s}{\sigma_j} \right) - \Phi\left(\frac{c_l - \delta_j - \beta_j f_s}{\sigma_j} \right) \right] \right],$$

where f_s is simulated $S = 500$ times from a standard normal distribution.

D.1. Figures for CL(1)

Figure 1: Empirical PDF for $\hat{c}_{k+1}$ when $\rho = 0$

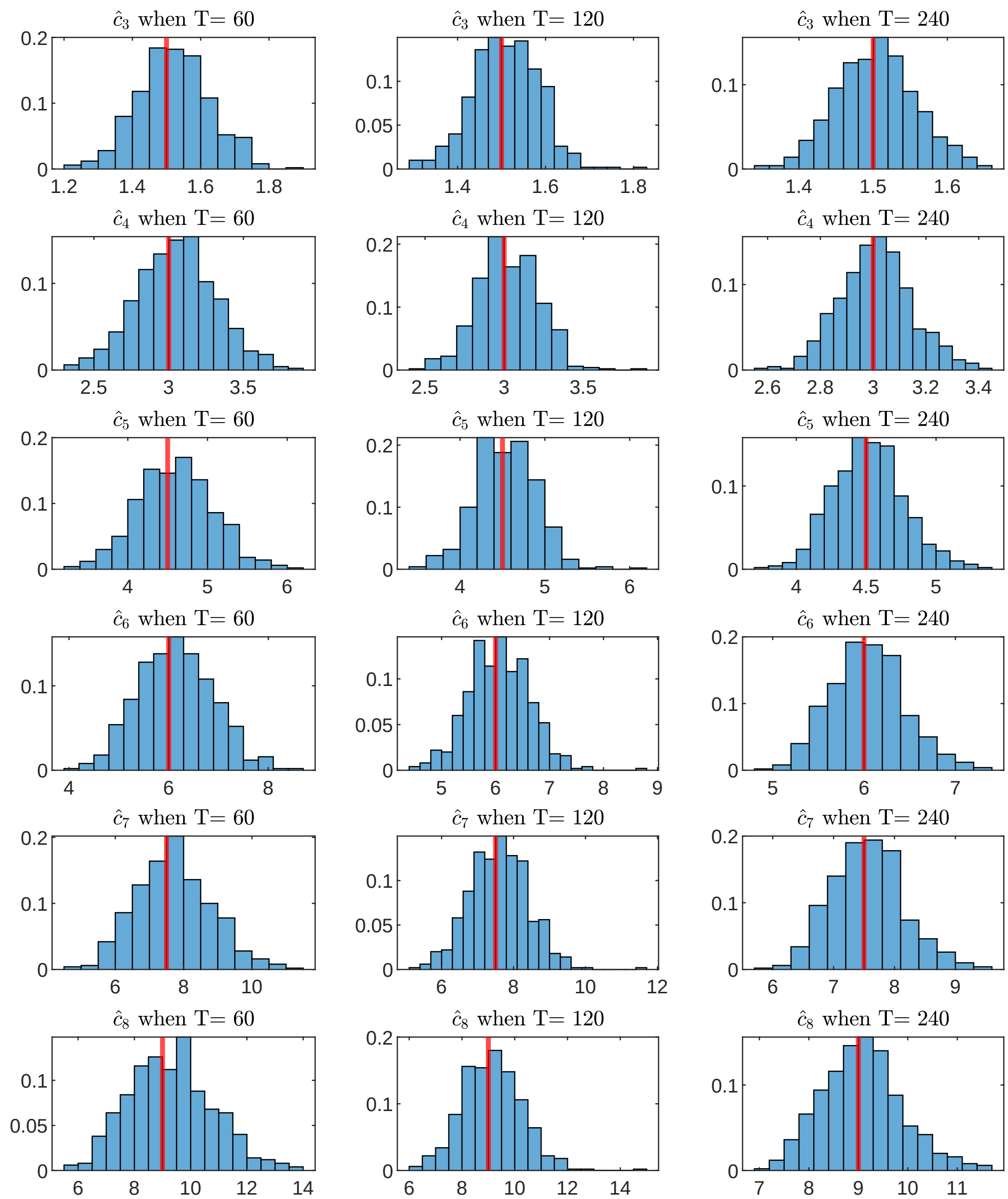

Figure 2: Empirical PDF for $\hat{c}_{k+1}$ when $\rho = 0.4$

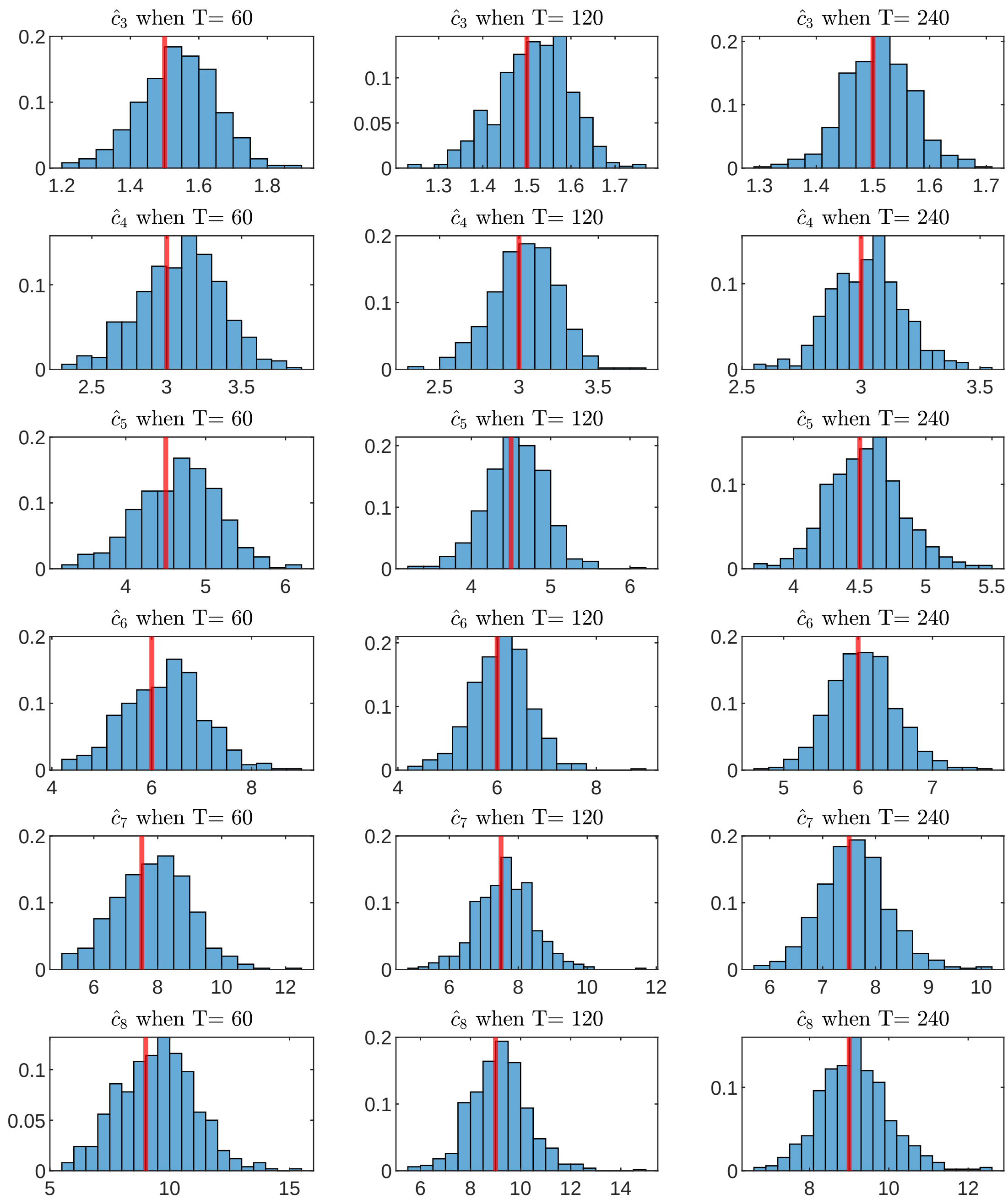

Figure 3: Empirical PDF for $\hat{c}_{k+1}$ when $\rho = 0.7$

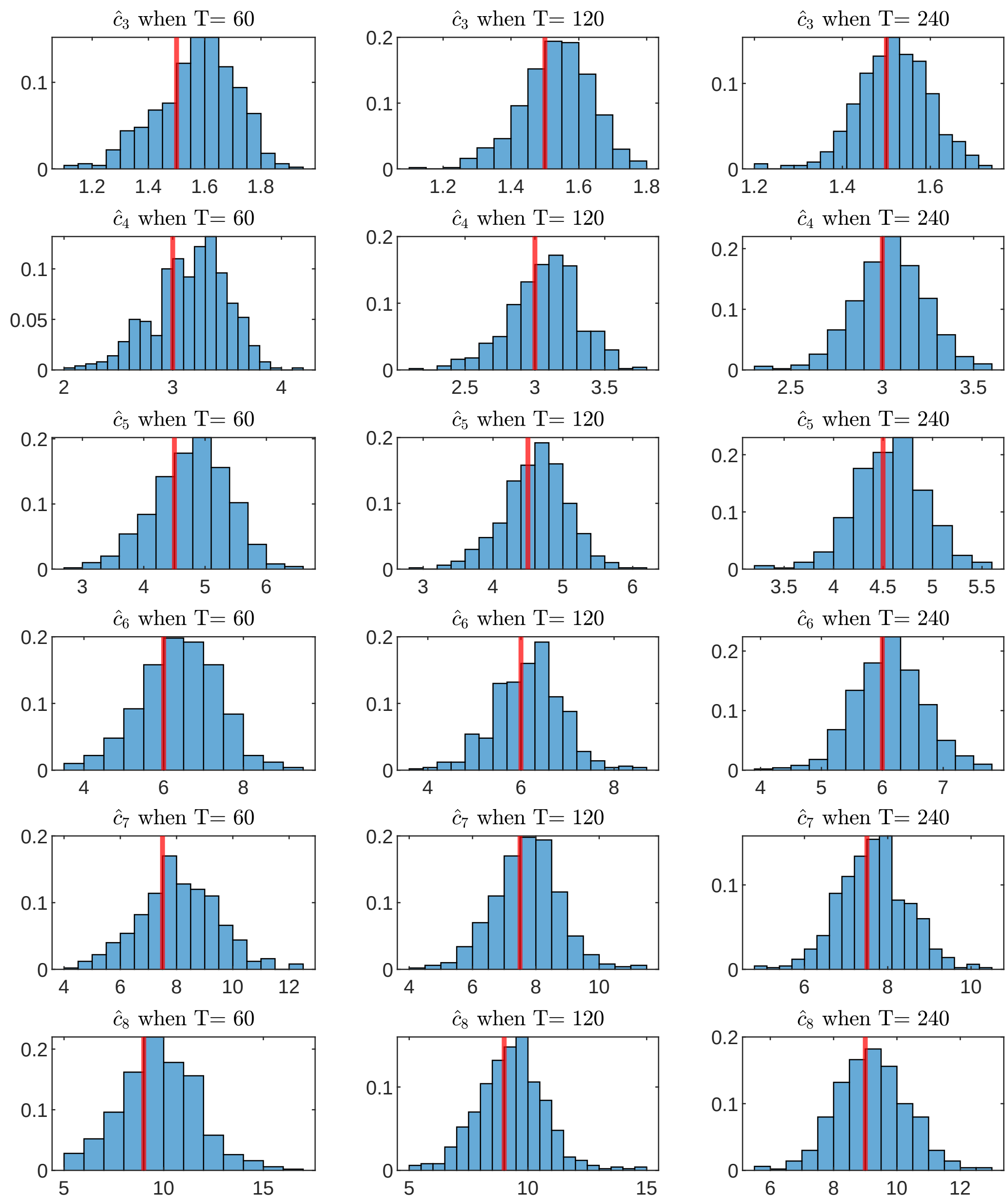

Figure 4: Empirical PDF for $\hat{c}_{k+1}$ when $\rho = 0.95$

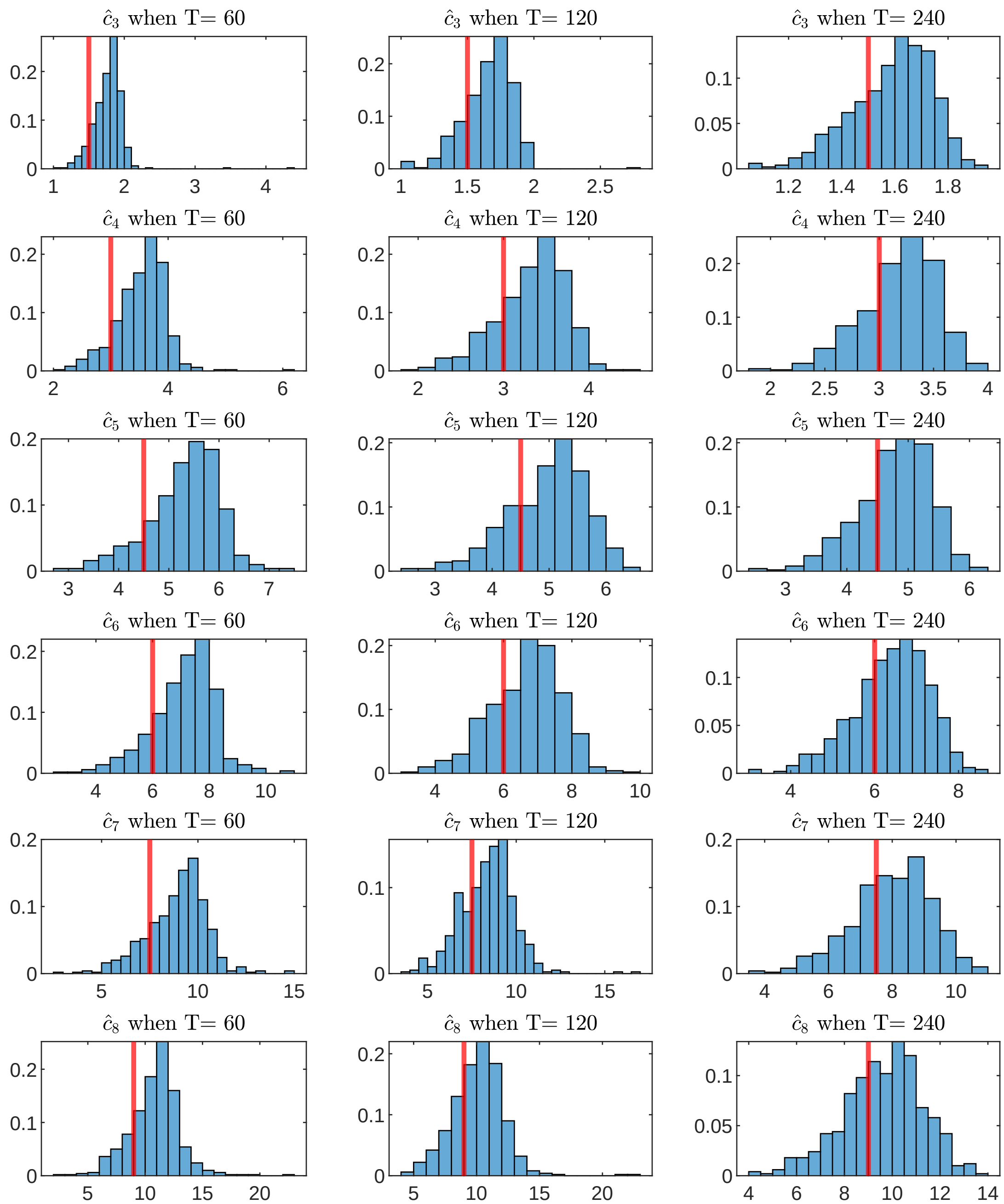

Figure 5: Empirical PDF for $\hat{\delta}_j$ when $\rho = 0$

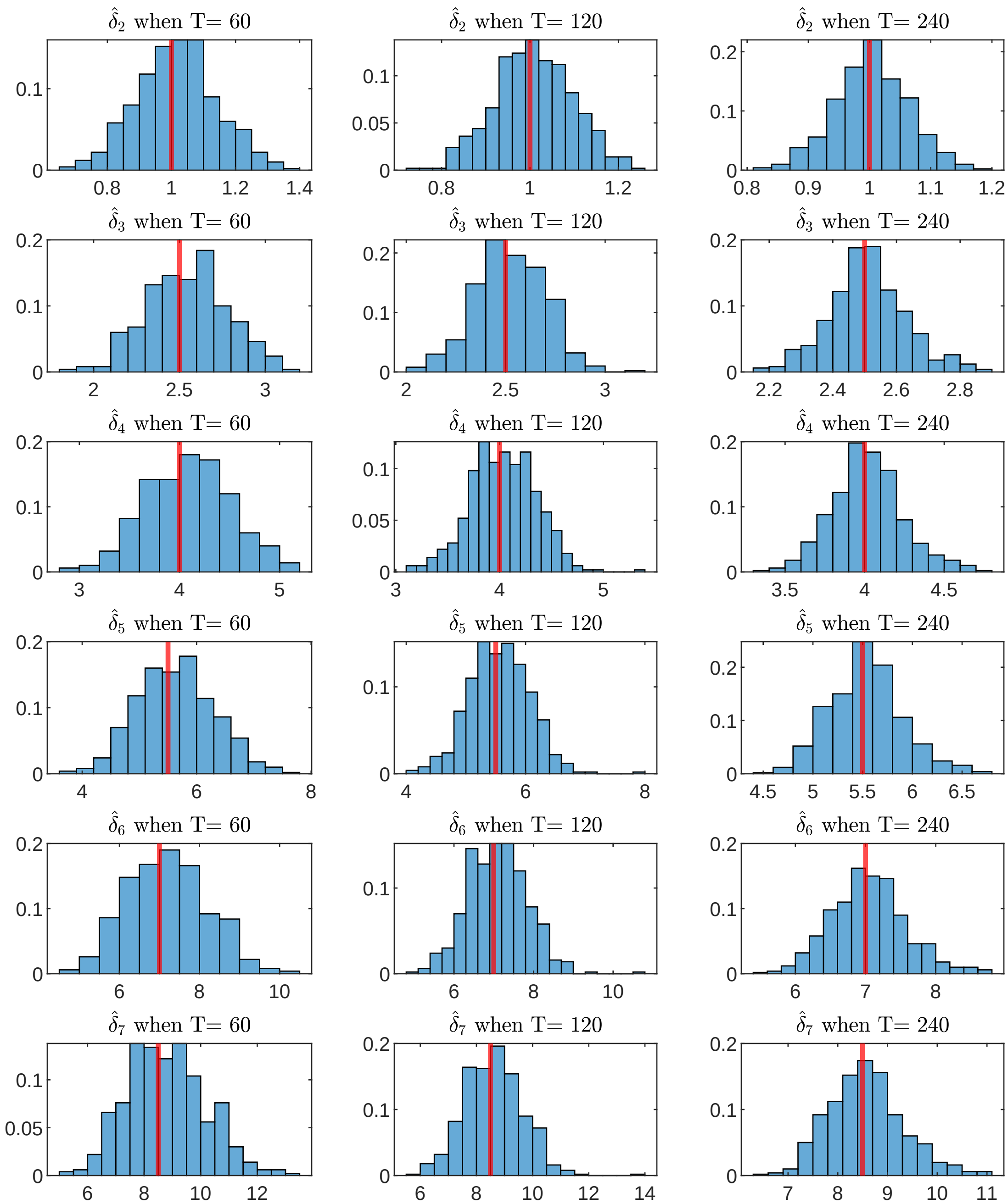

Figure 6: Empirical PDF for $\hat{\delta}_j$ when $\rho = 0.4$

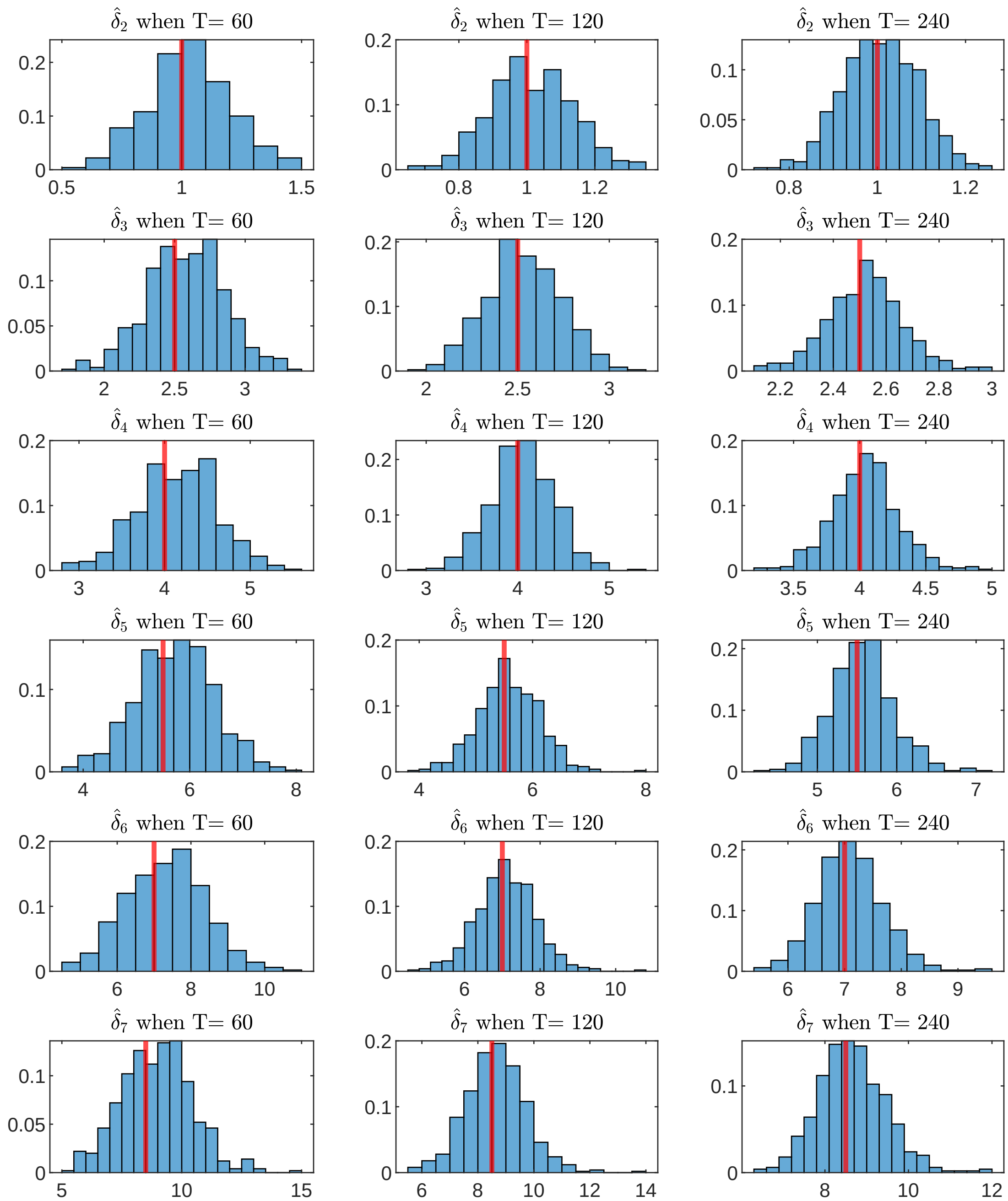

Figure 7: Empirical PDF for $\hat{\delta}_j$ when $\rho = 0.7$

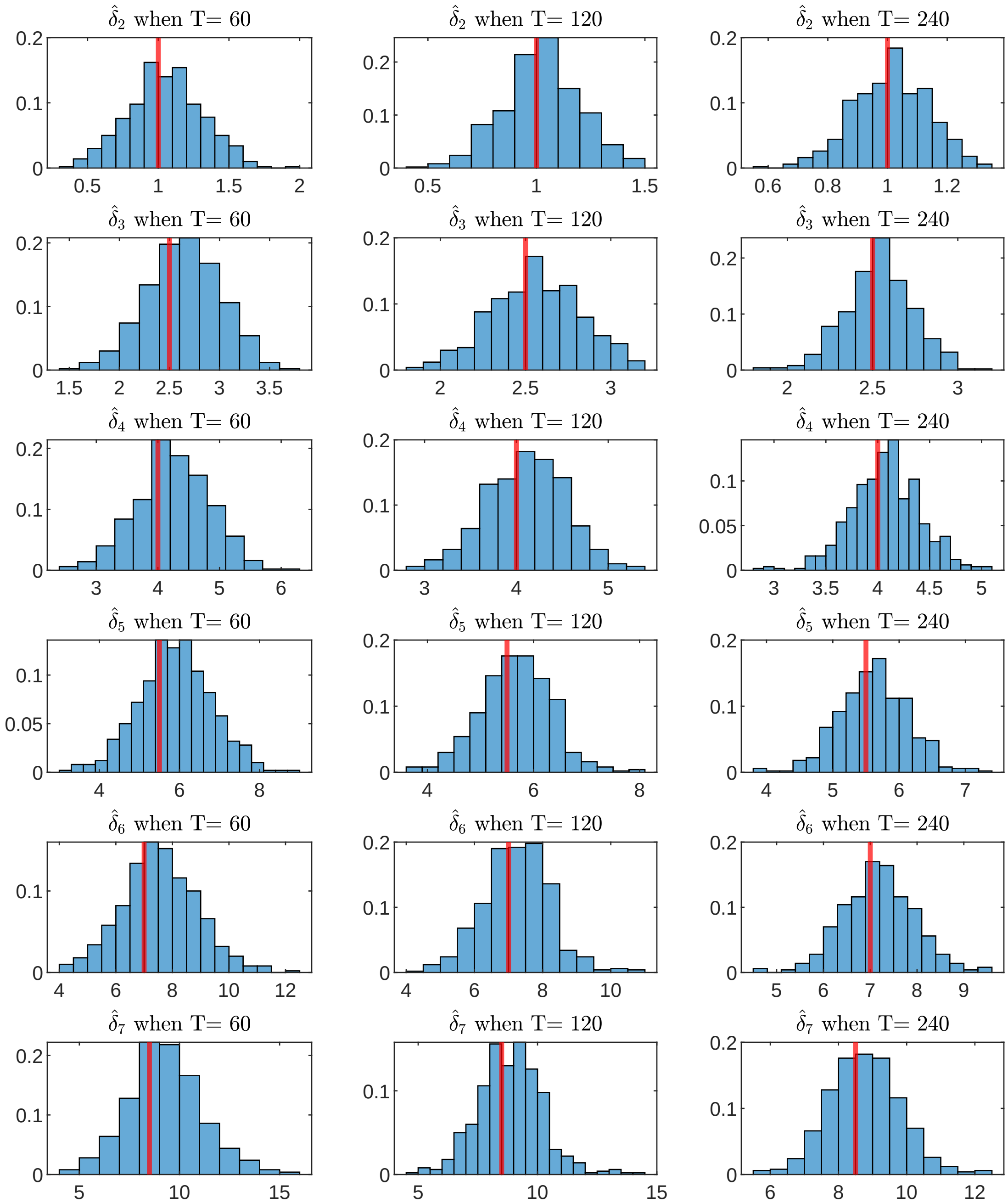

Figure 8: Empirical PDF for $\hat{\delta}_j$ when $\rho = 0.95$

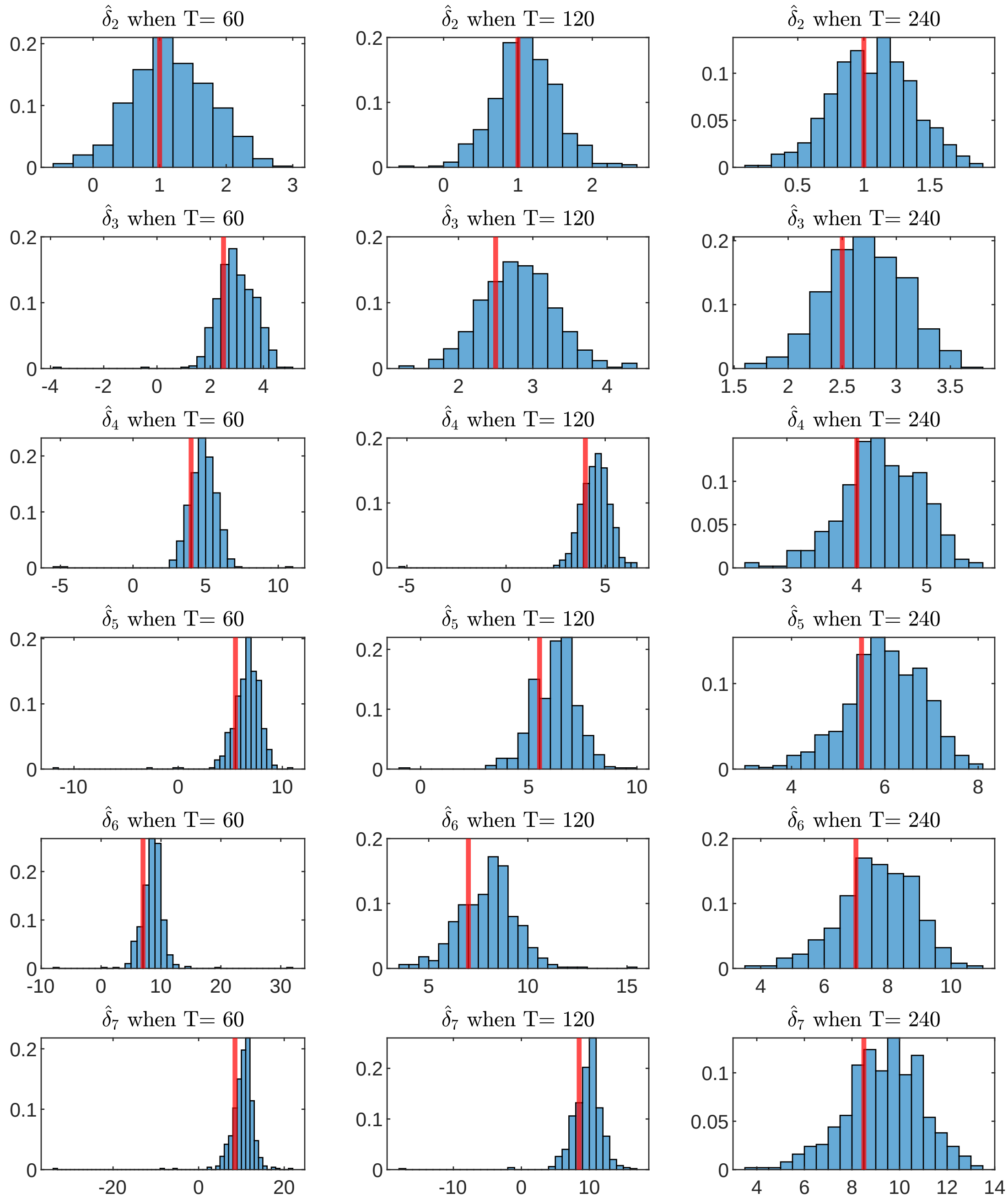

Figure 9: Empirical PDF for $\hat{\gamma}_j$ when $\rho = 0$

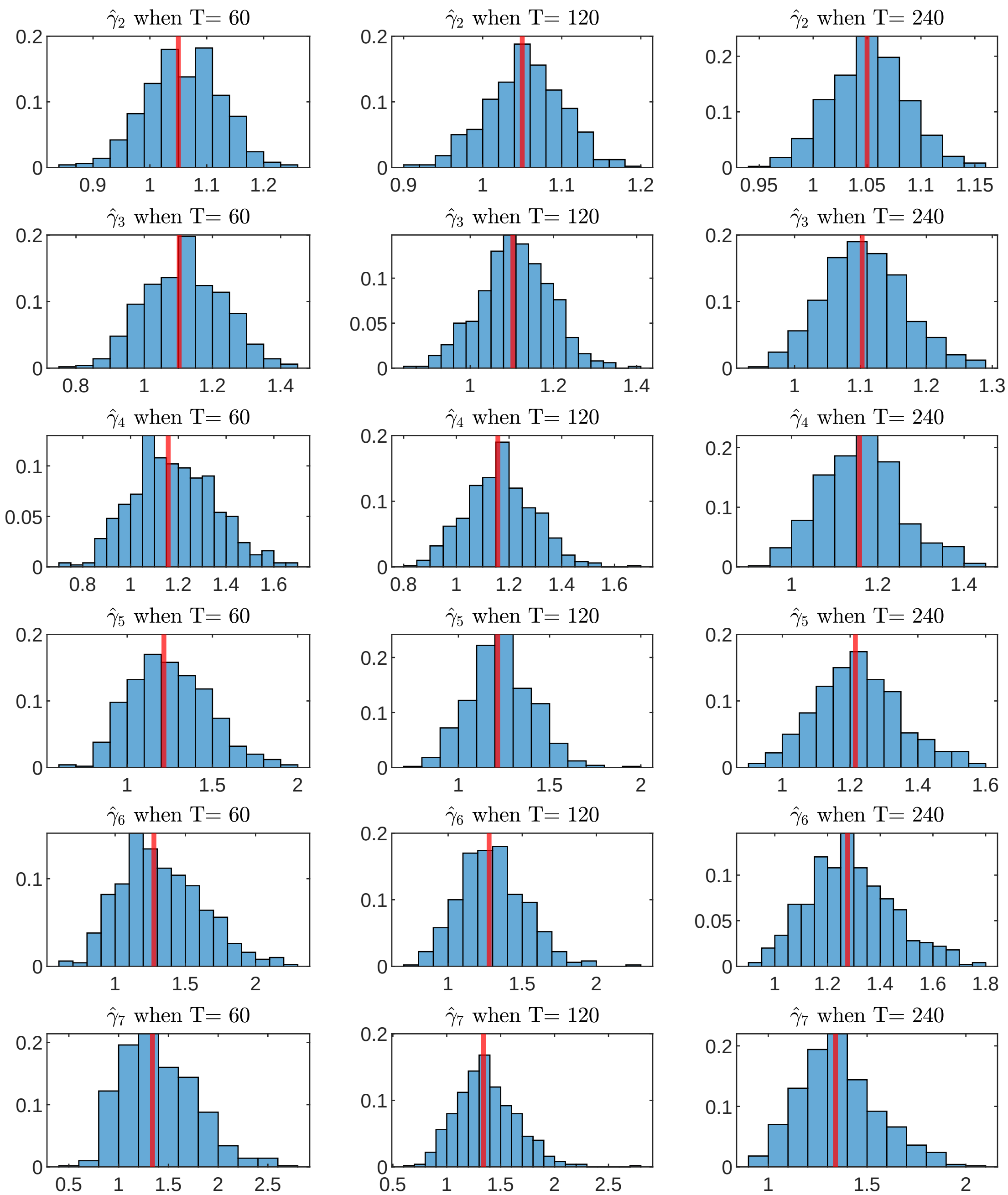

Figure 10: Empirical PDF for $\hat{\gamma}_j$ when $\rho = 0.4$

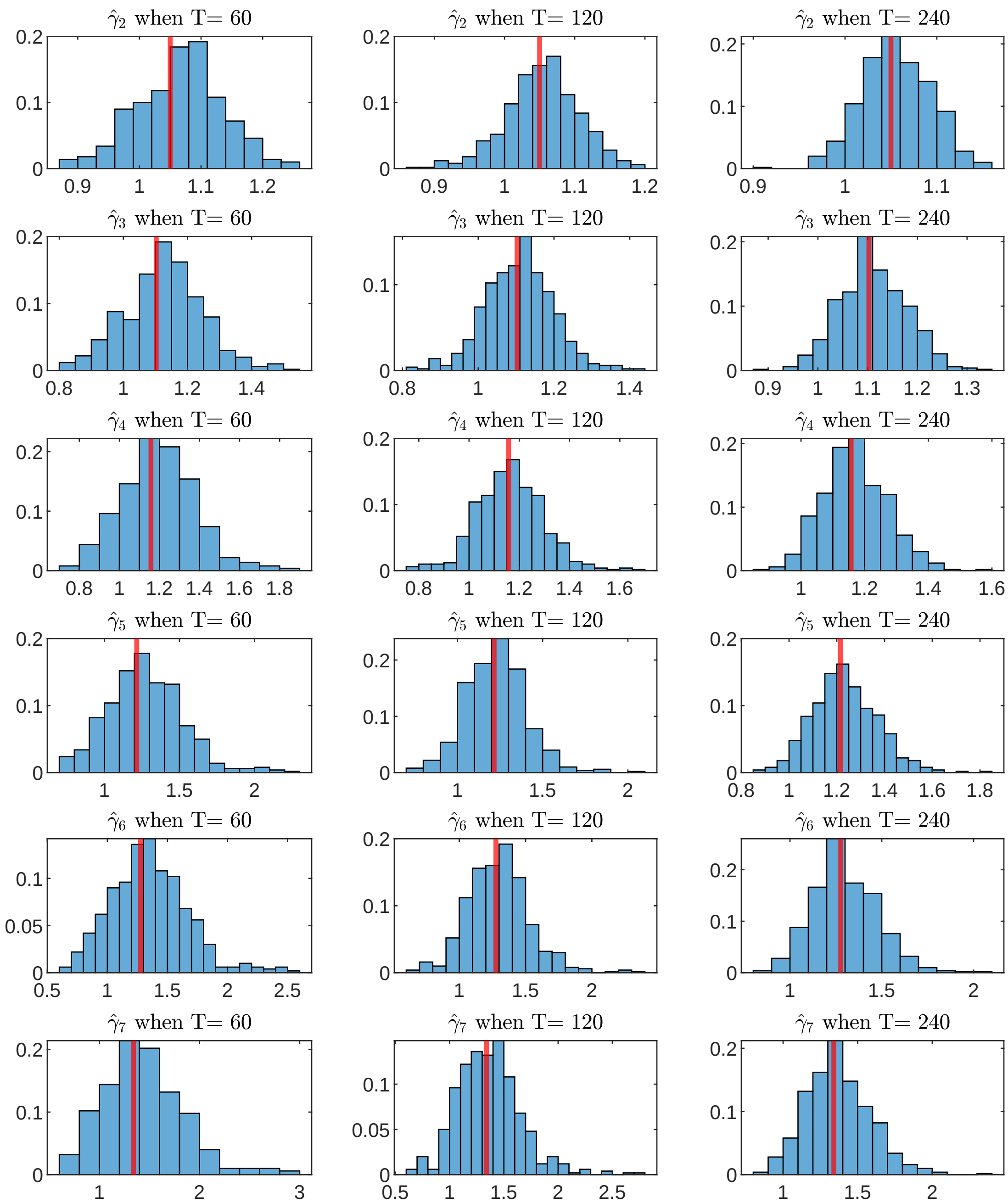

Figure 11: Empirical PDF for $\hat{\gamma}_j$ when $\rho = 0.7$

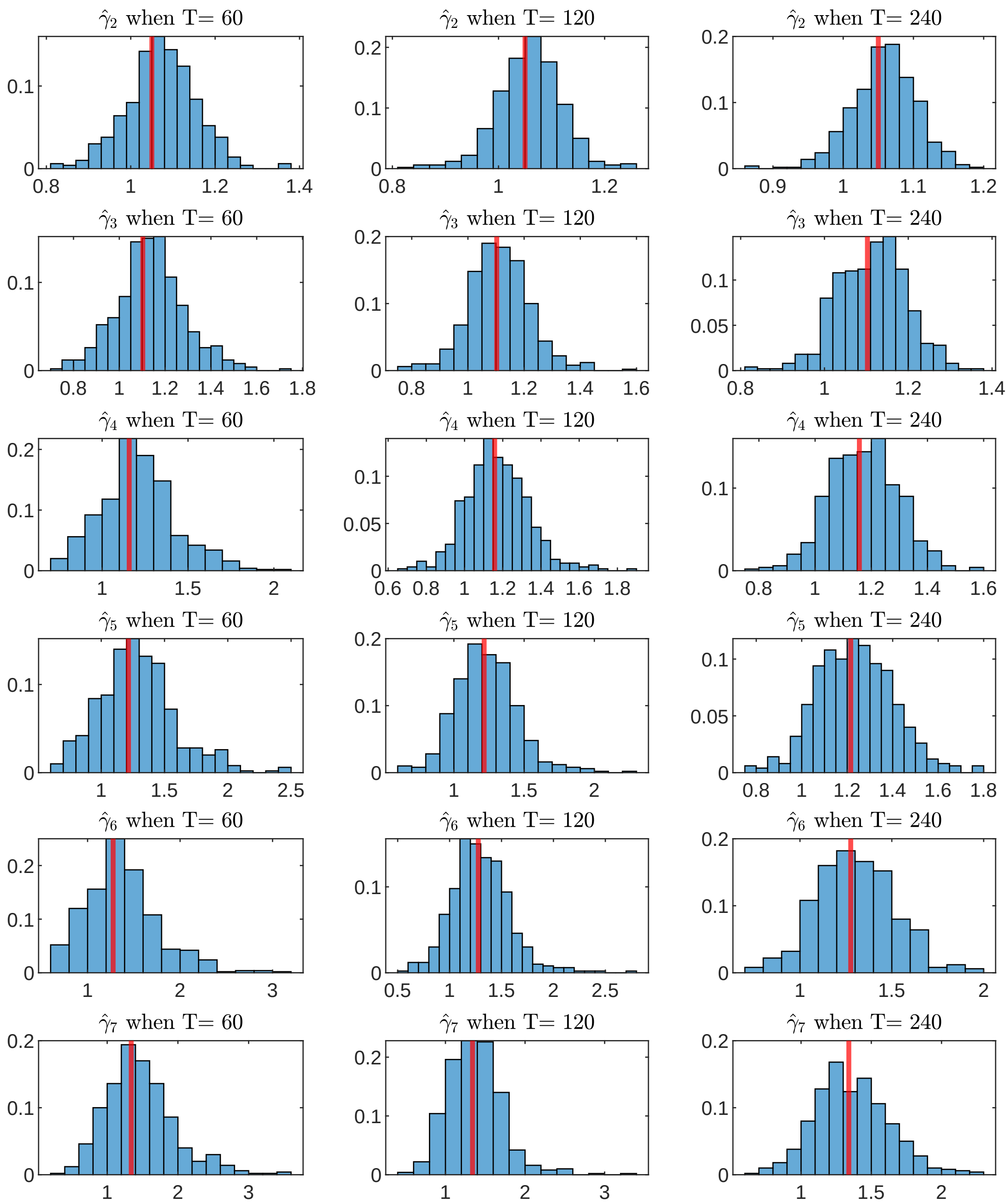

Figure 12: Empirical PDF for $\hat{\gamma}_j$ when $\rho = 0.95$

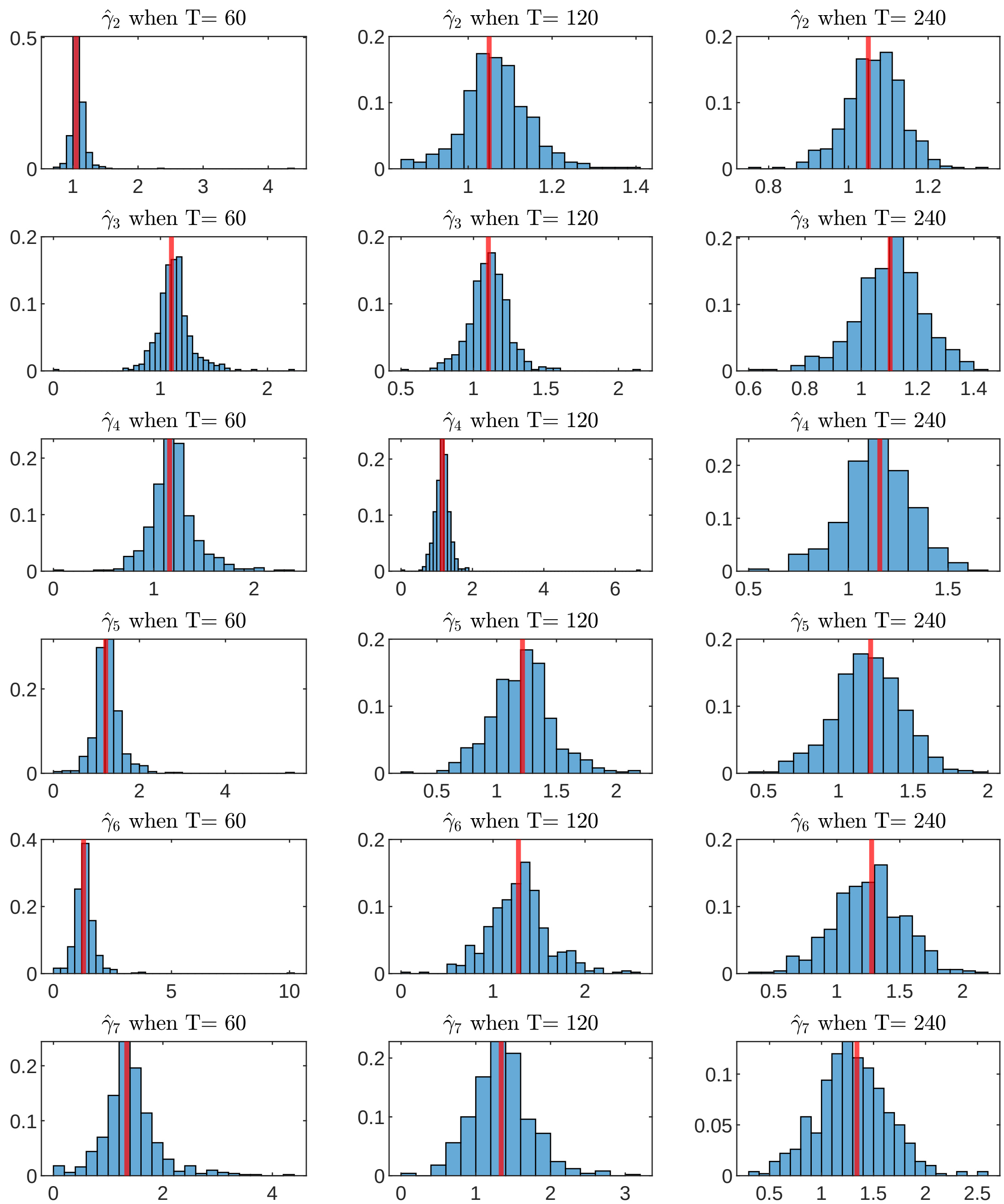

D.2. Figures for CL(2)

Figure 13: Empirical PDF for $\hat{c}_{k+1}$ when $\rho = 0$

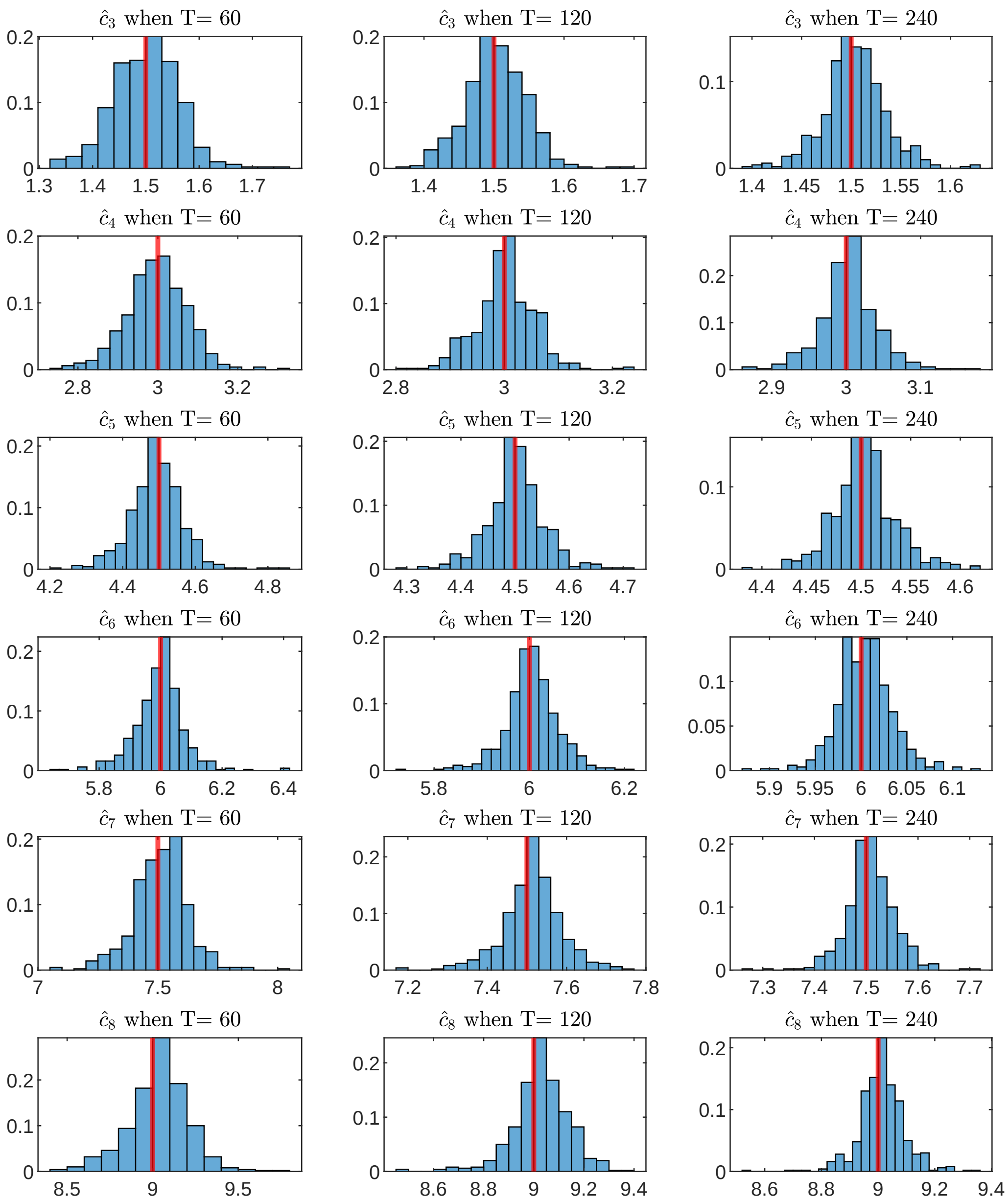

Figure 14: Empirical PDF for $\hat{c}_{k+1}$ when $\rho = 0.4$

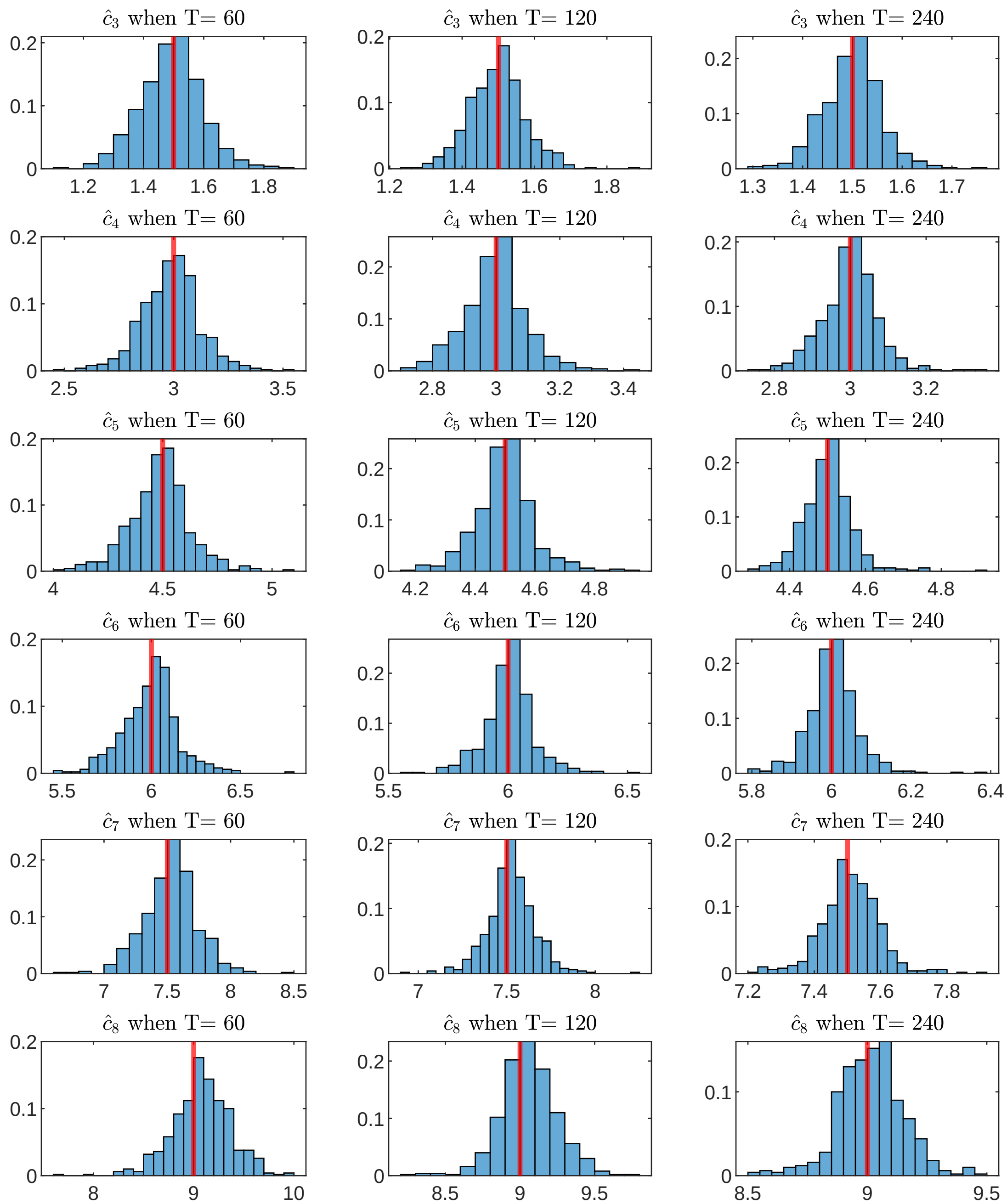

Figure 15: Empirical PDF for $\hat{c}_{k+1}$ when $\rho = 0.7$

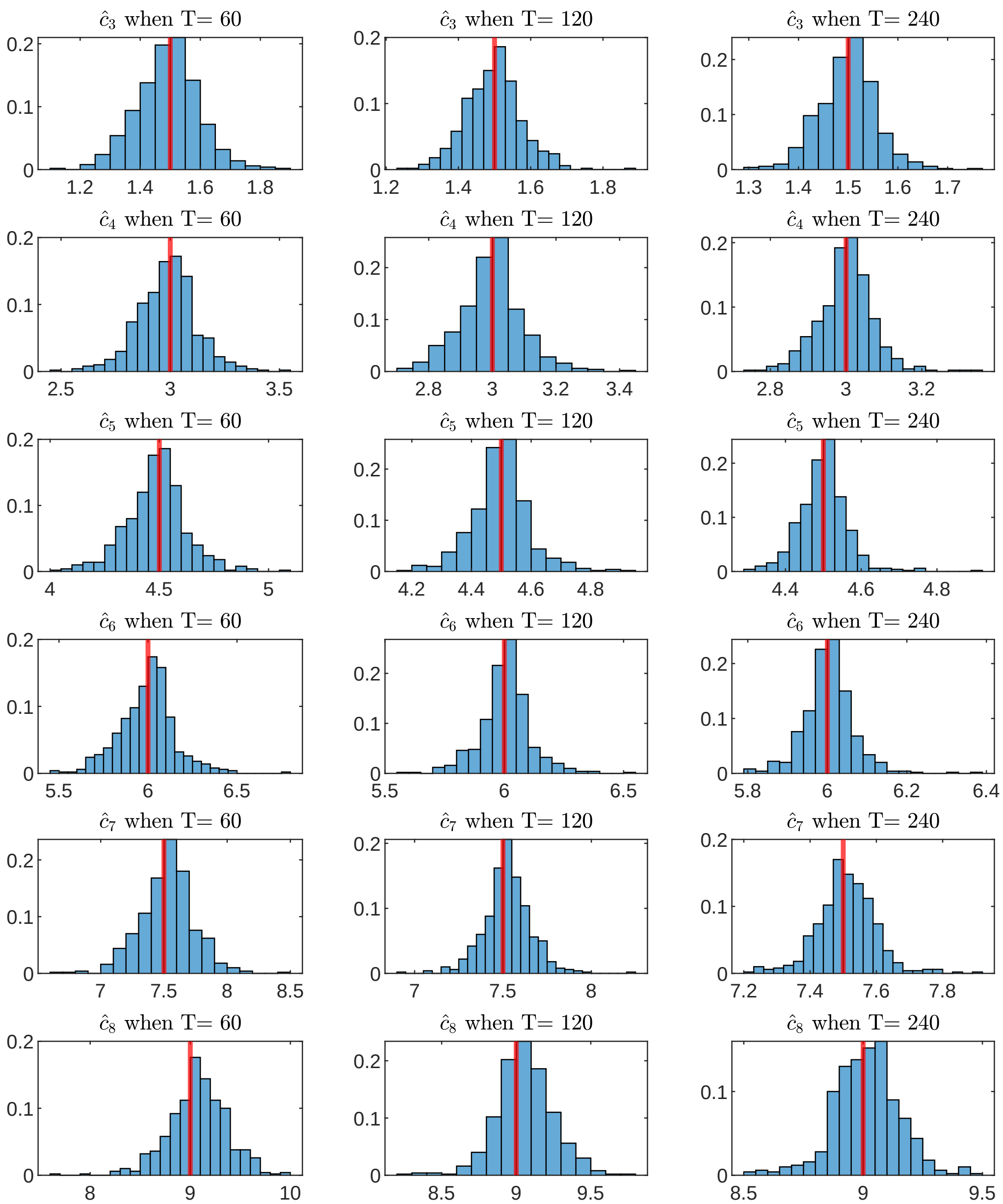

Figure 16: Empirical PDF for $\hat{c}_{k+1}$ when $\rho = 0.95$

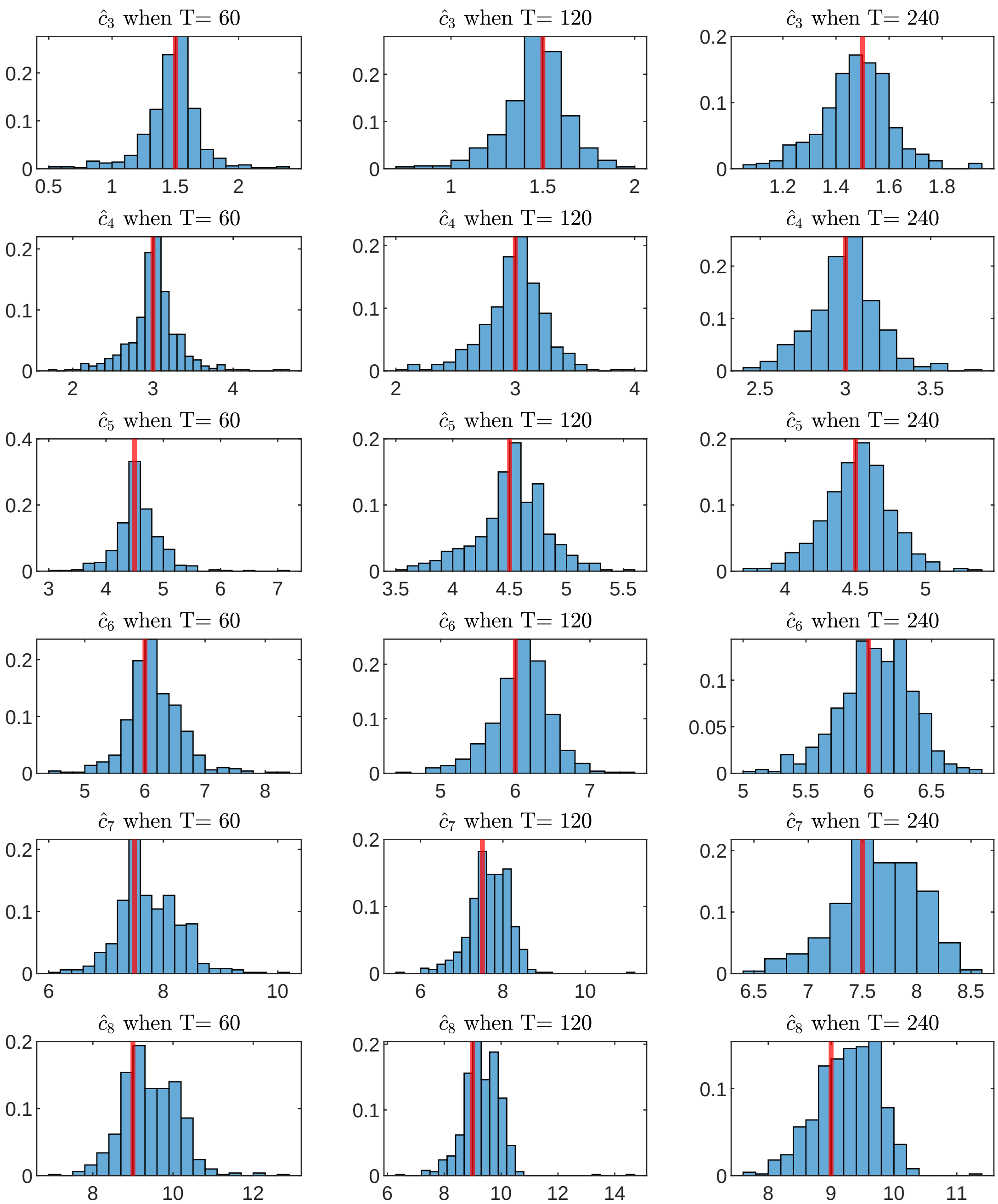

Figure 17: Empirical PDF for $\hat{\delta}_j$ when $\rho = 0$

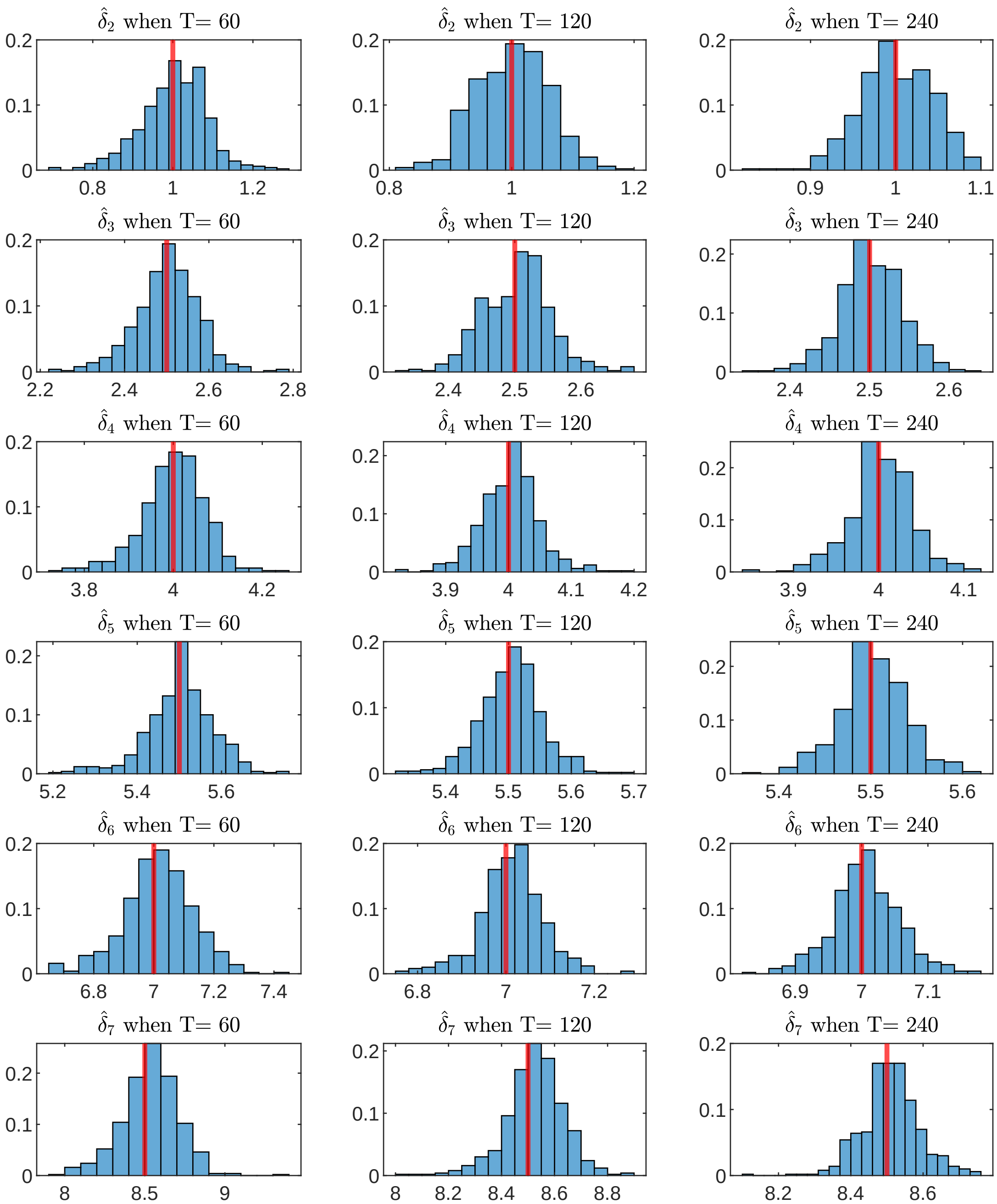

Figure 18: Empirical PDF for $\hat{\delta}_j$ when $\rho = 0.4$

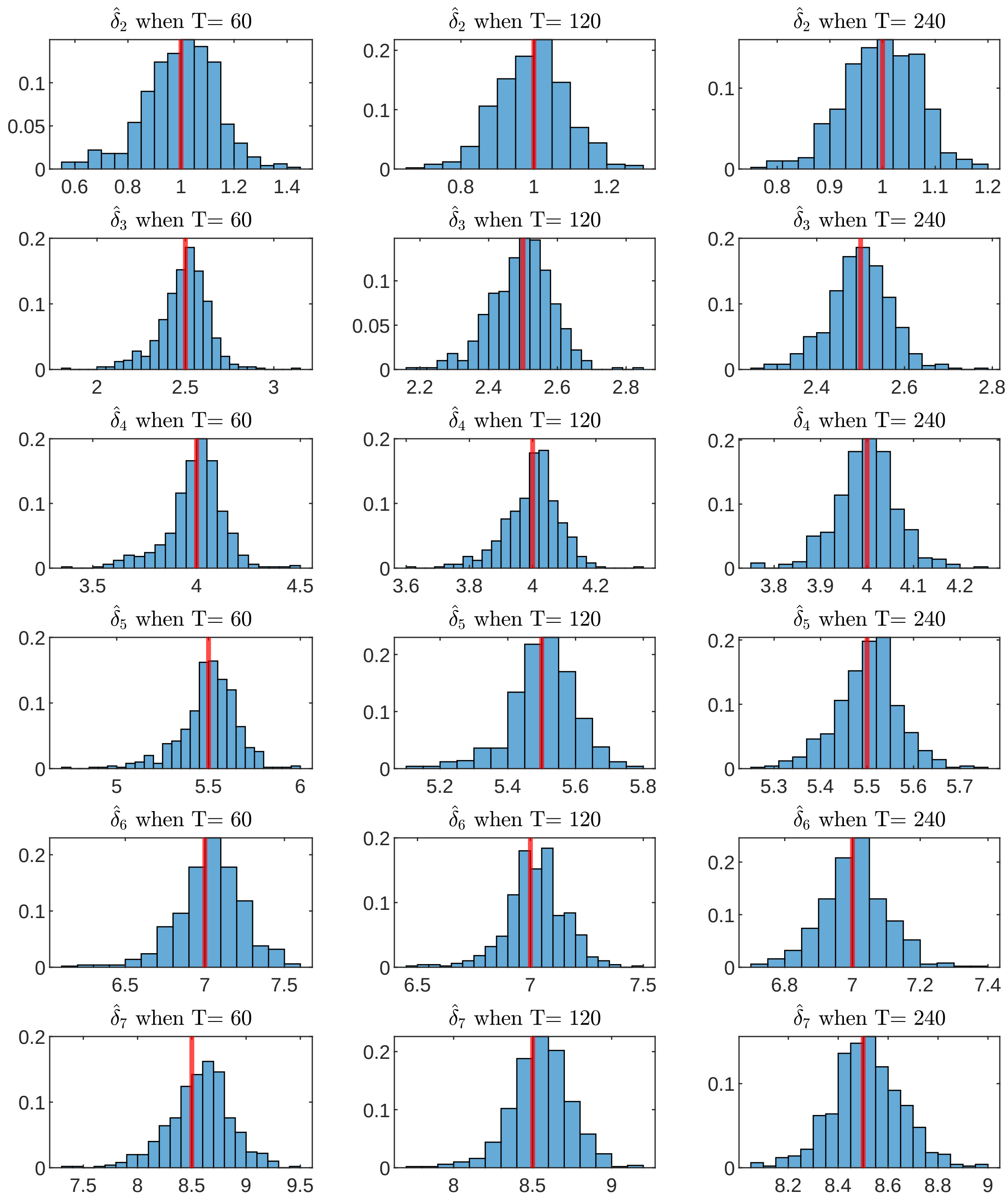

Figure 19: Empirical PDF for $\hat{\delta}_j$ when $\rho = 0.7$

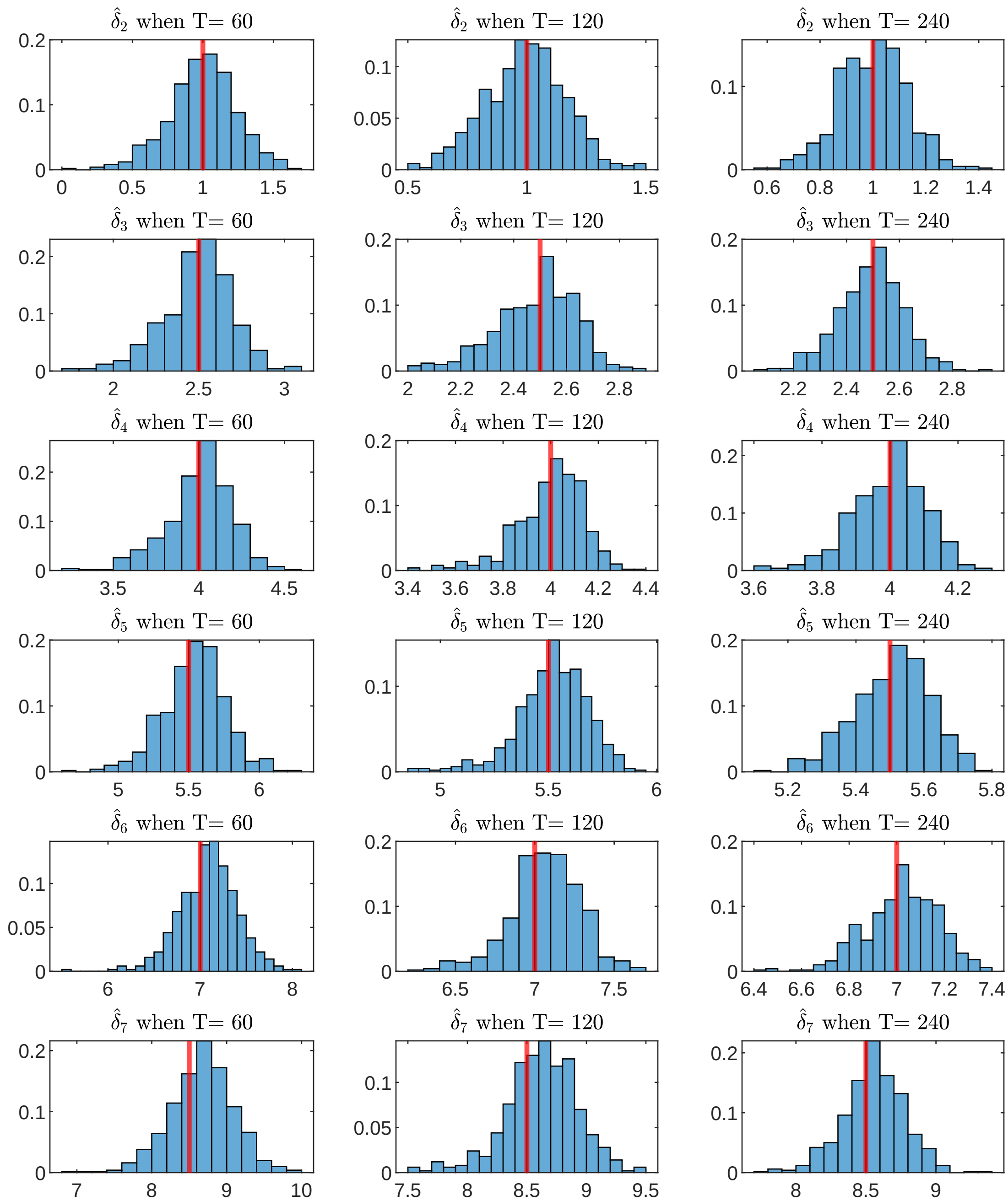

Figure 20: Empirical PDF for $\hat{\delta}_j$ when $\rho = 0.95$

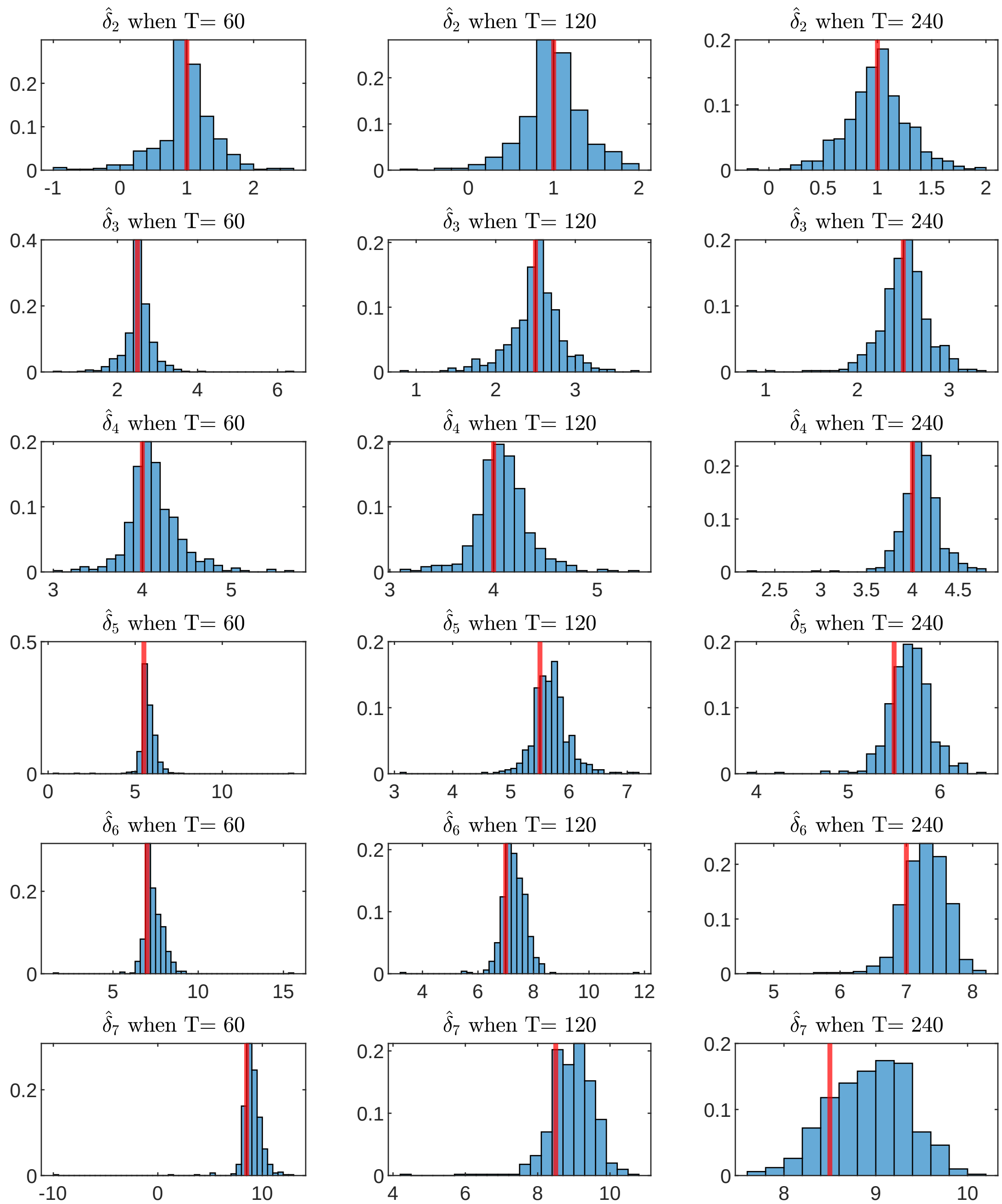

Figure 21: Empirical PDF for $\hat{\beta}_j$ when $\rho = 0$

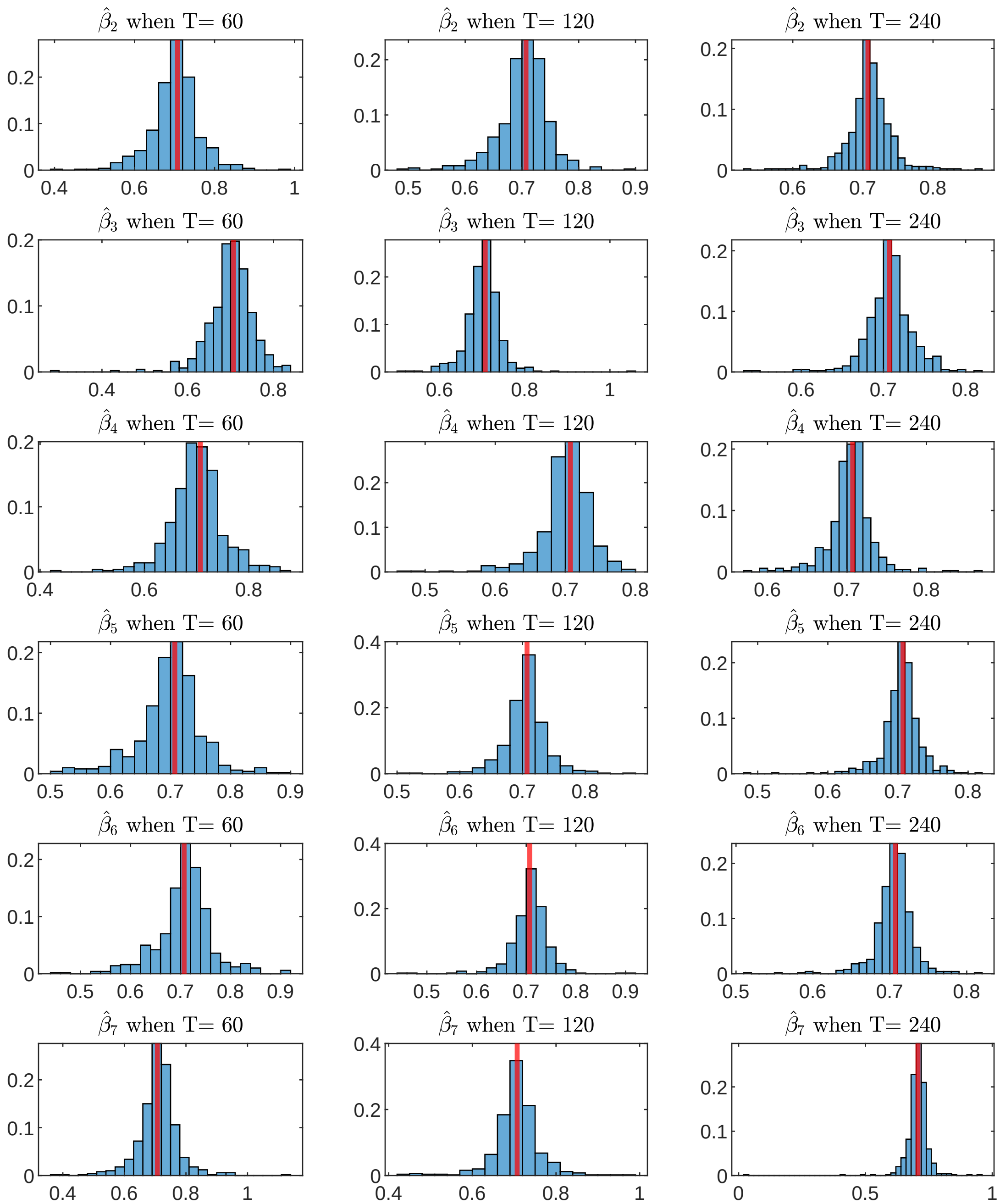

Figure 22: Empirical PDF for $\hat{\beta}_j$ when $\rho = 0.4$

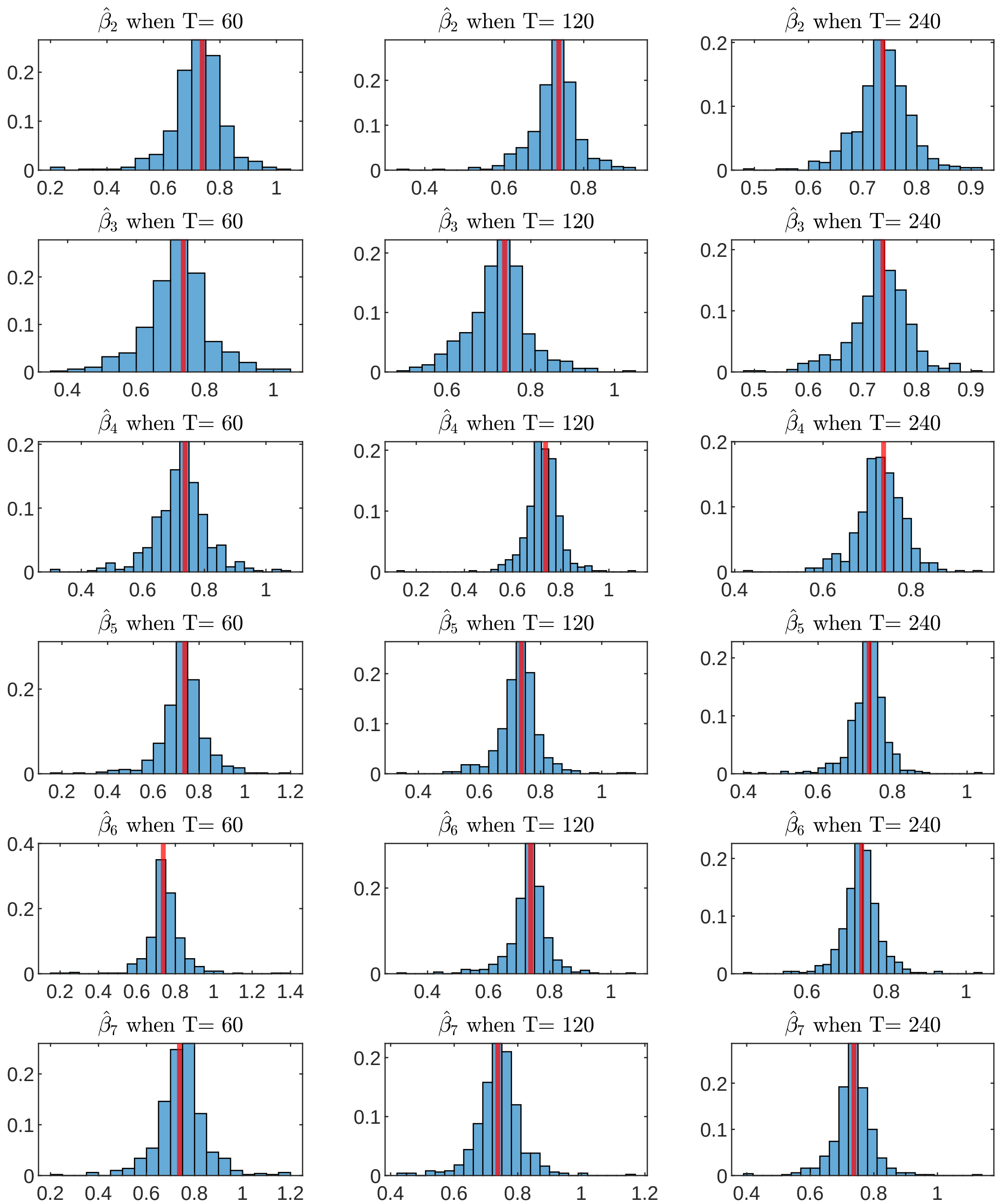

Figure 23: Empirical PDF for $\hat{\beta}_j$ when $\rho = 0.7$

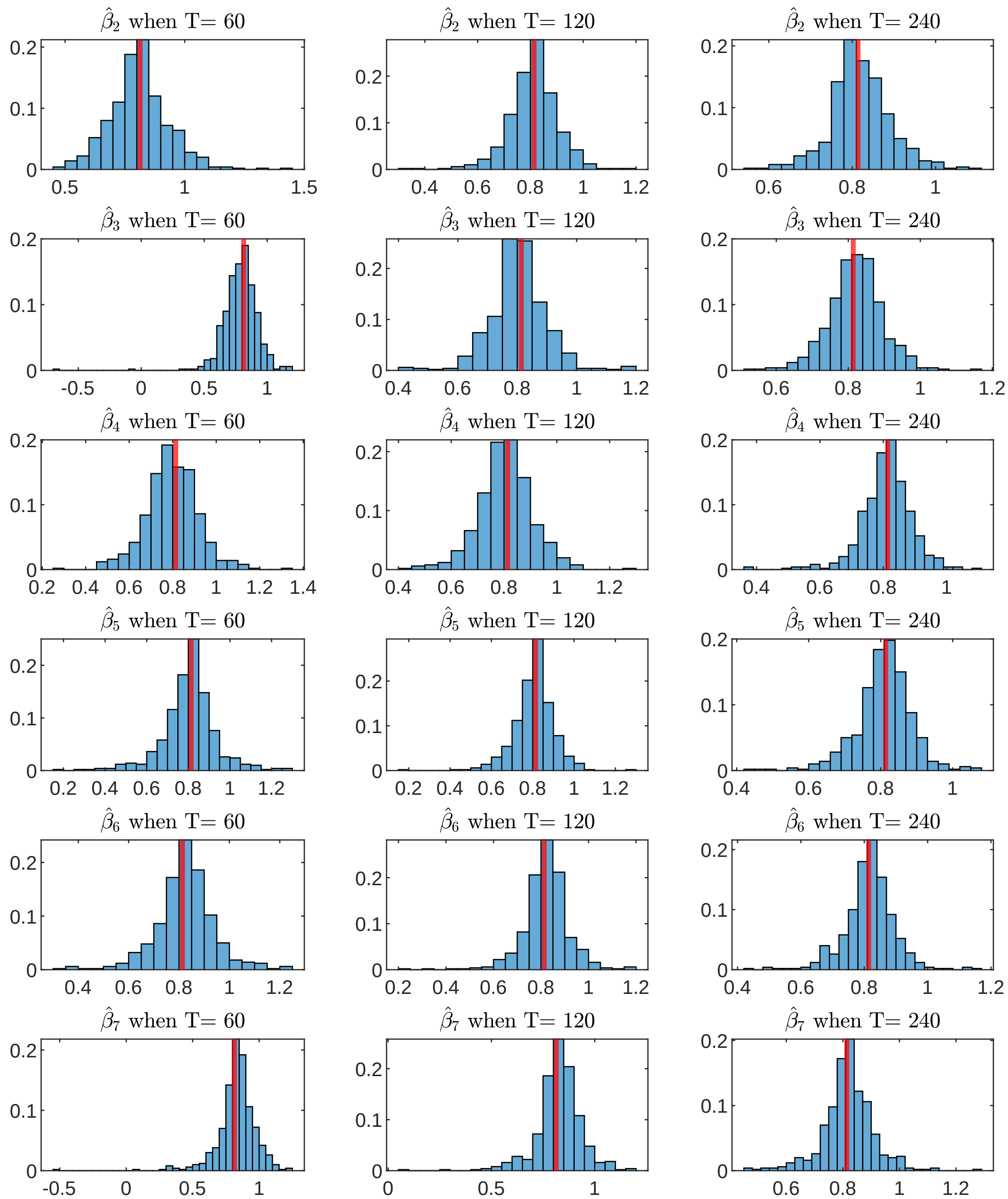

Figure 24: Empirical PDF for $\hat{\beta}_j$ when $\rho = 0.95$

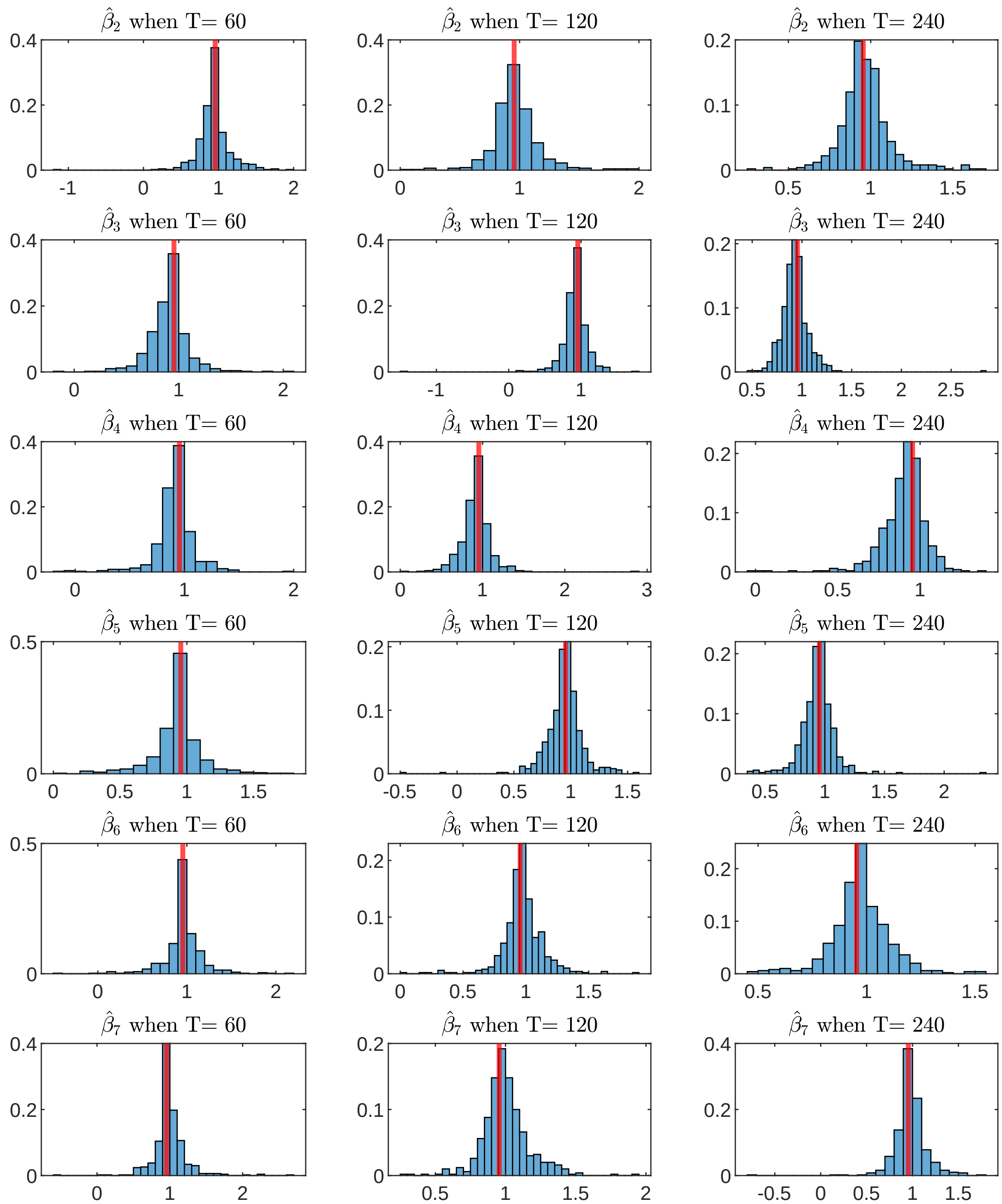

Figure 25: Empirical PDF for $\hat{\sigma}_j$ when $\rho = 0$

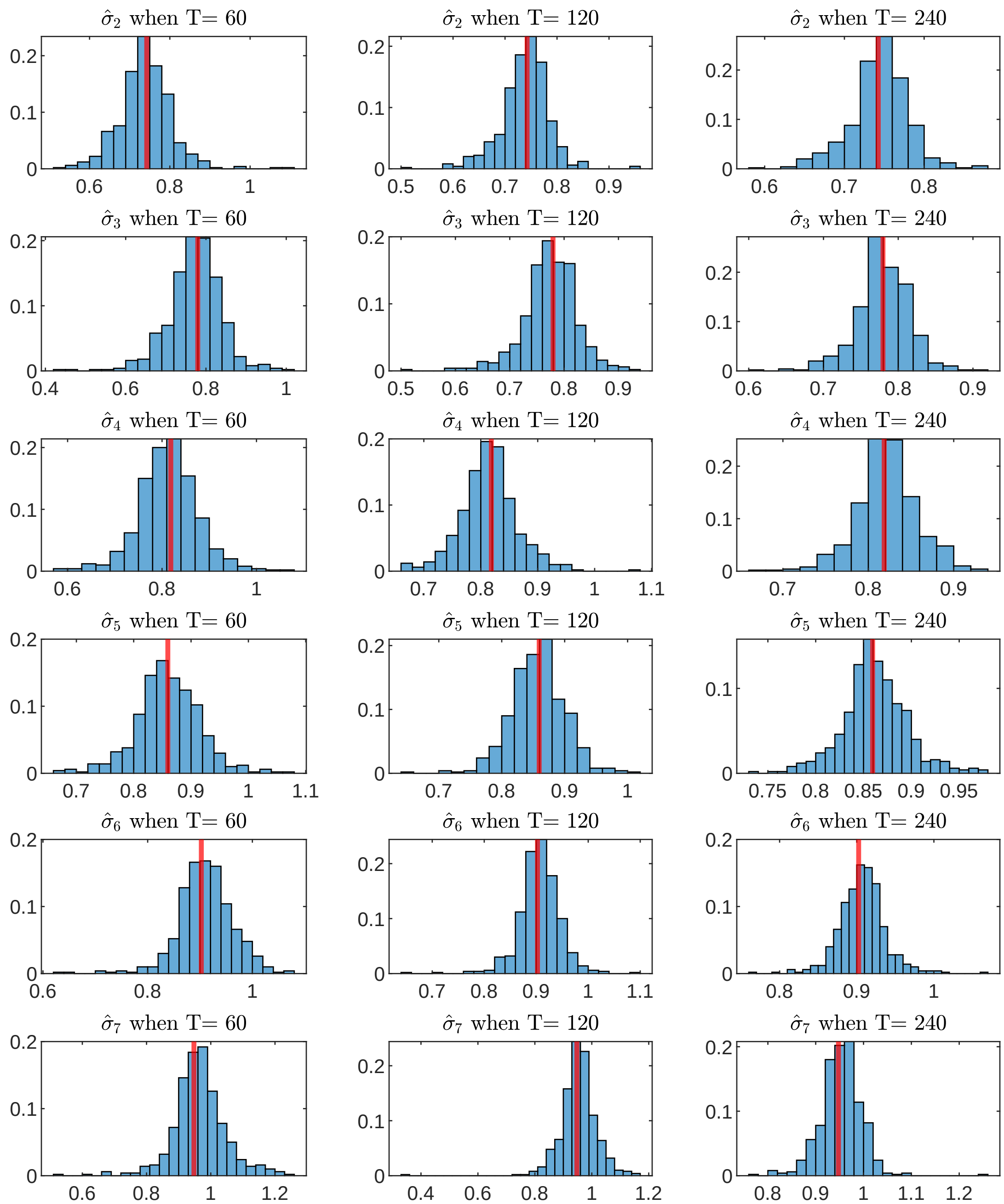

Figure 26: Empirical PDF for $\hat{\sigma}_j$ when $\rho = 0.4$

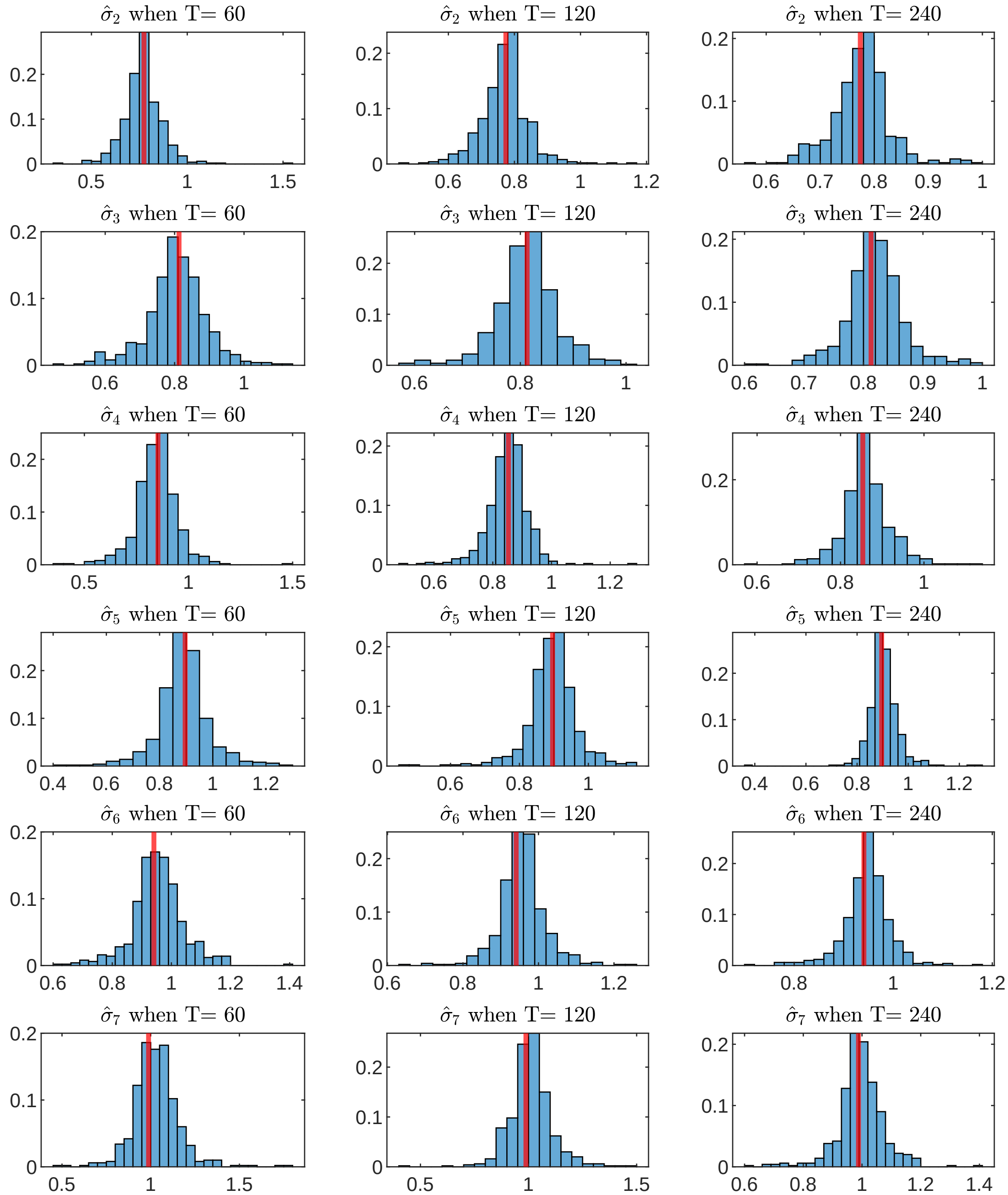

Figure 27: Empirical PDF for $\hat{\sigma}_j$ when $\rho = 0.7$

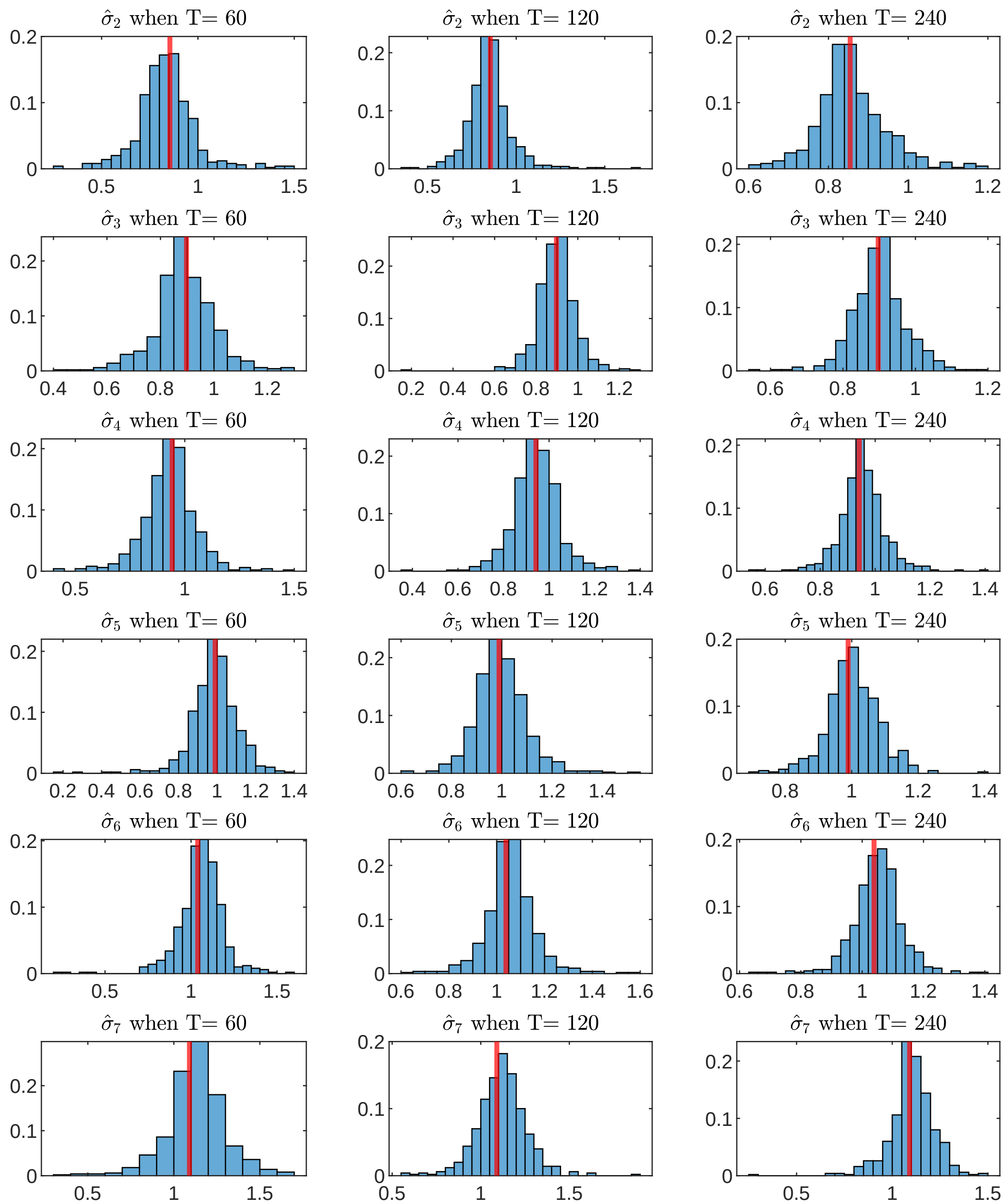

Figure 28: Empirical PDF for $\hat{\sigma}_j$ when $\rho = 0.95$

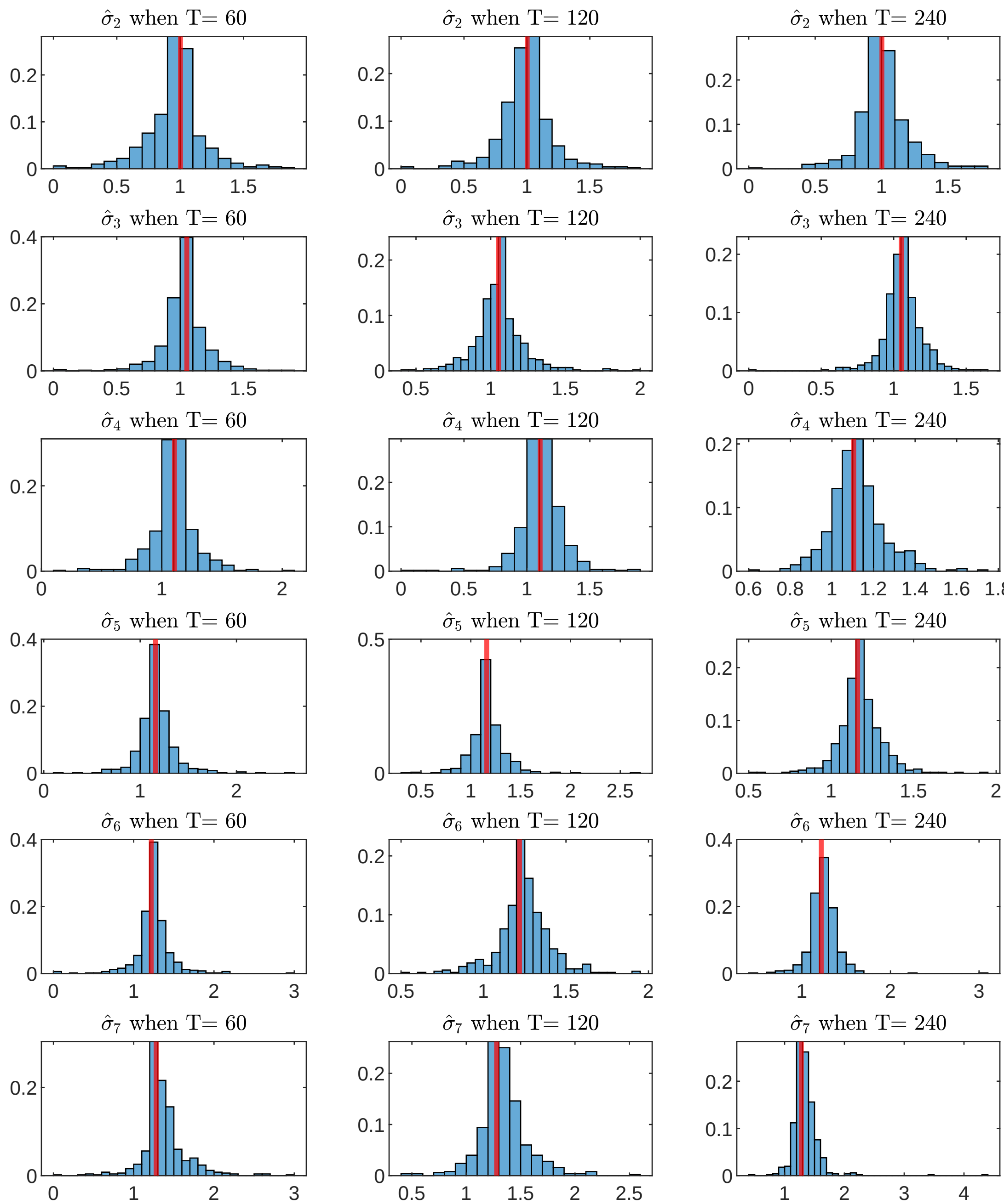

D.3. Figures for Granularity Approach

Figure 29: Empirical PDF for $\hat{c}_{k+1}$ when $\rho = 0$

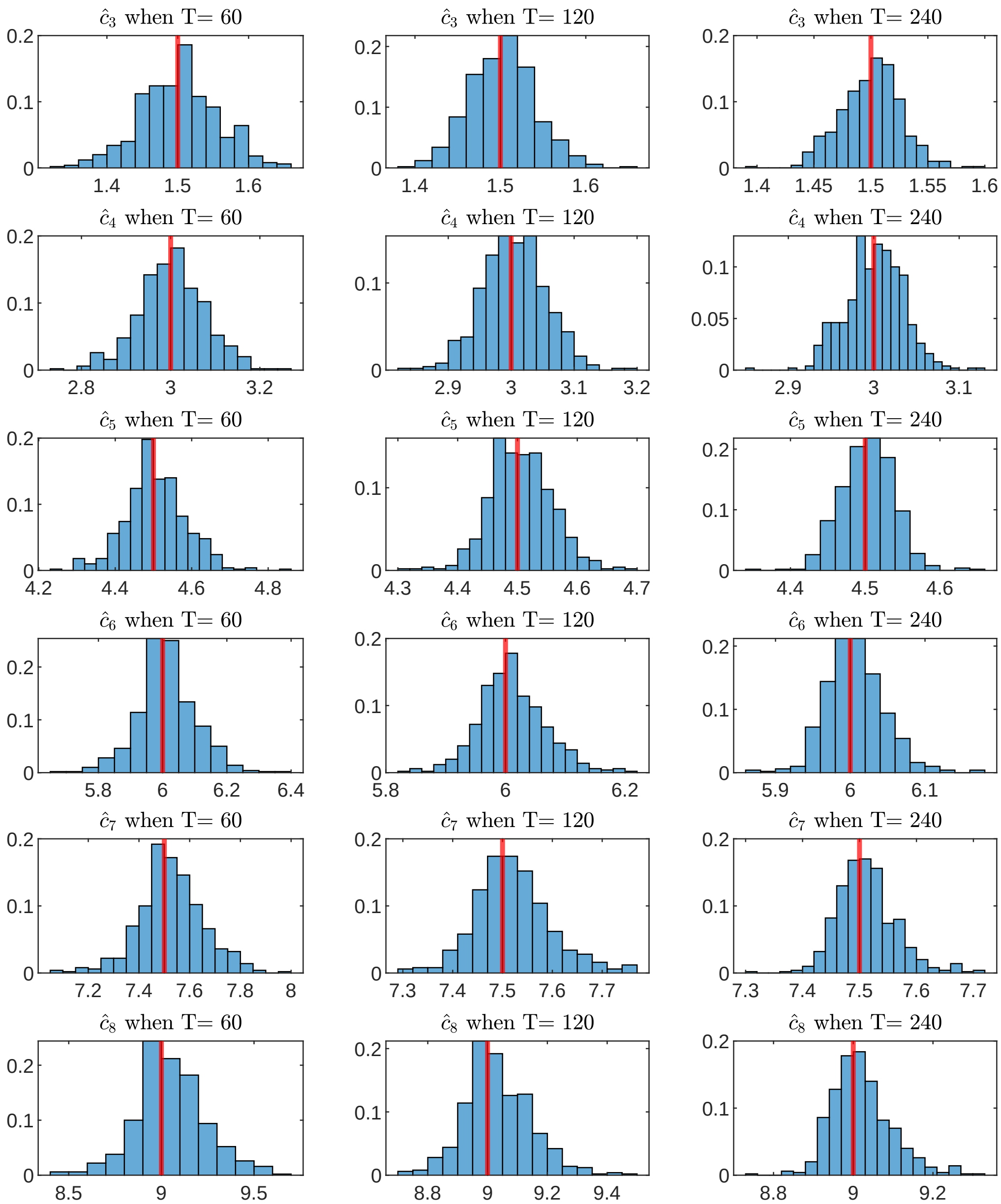

Figure 30: Empirical PDF for $\hat{c}_{k+1}$ when $\rho = 0.4$

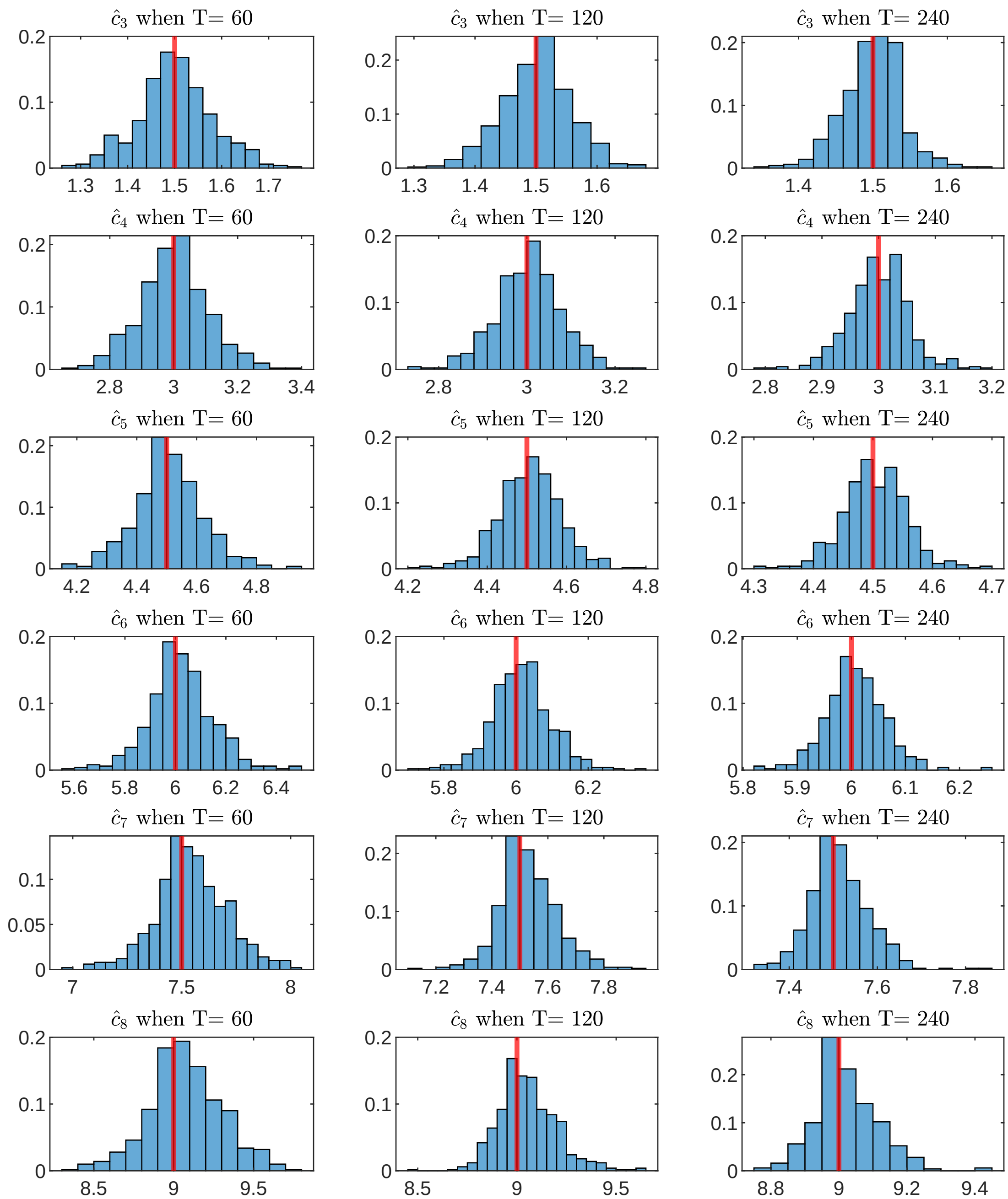

Figure 31: Empirical PDF for $\hat{c}_{k+1}$ when $\rho = 0.7$

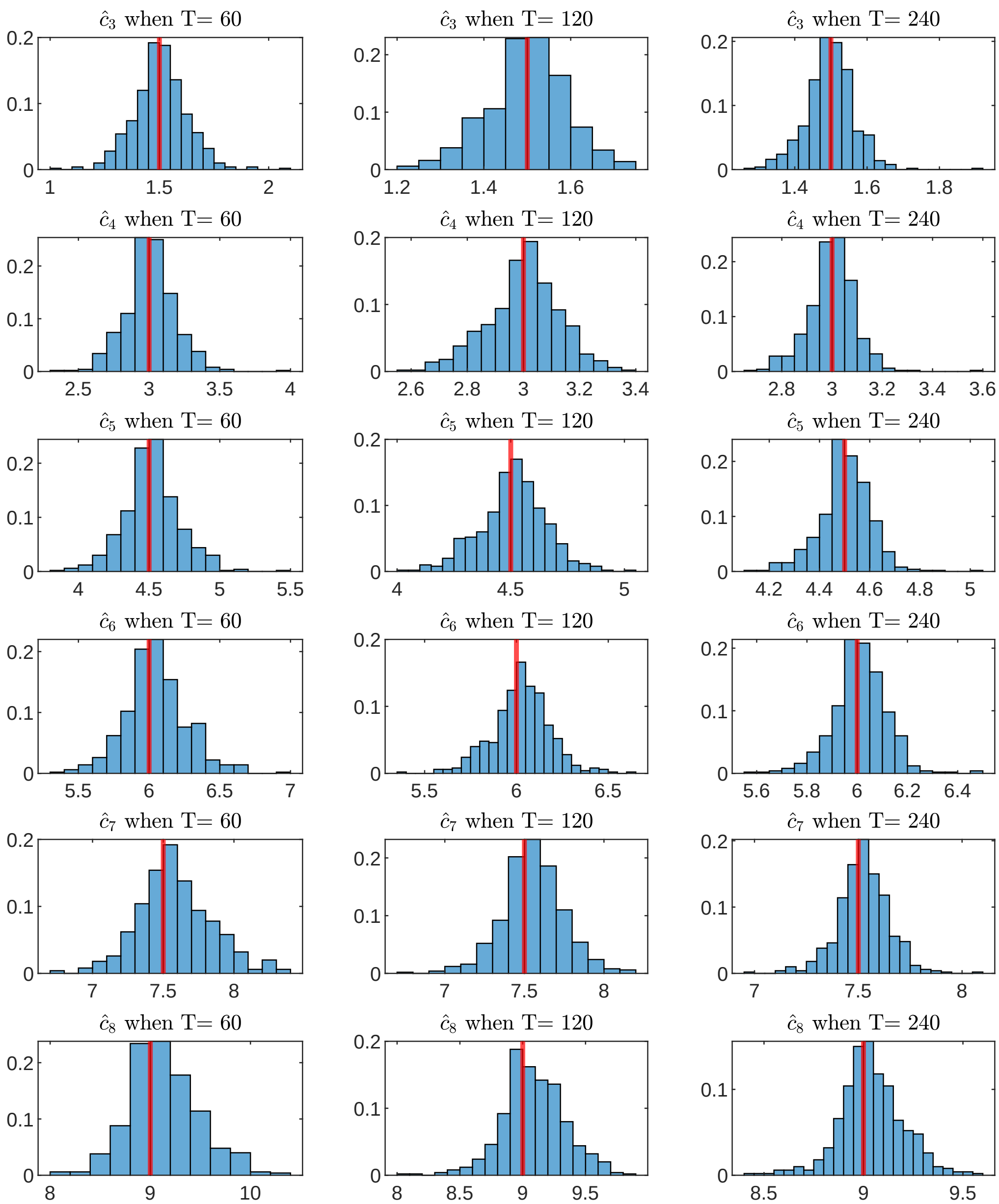

Figure 32: Empirical PDF for $\hat{c}_{k+1}$ when $\rho = 0.95$

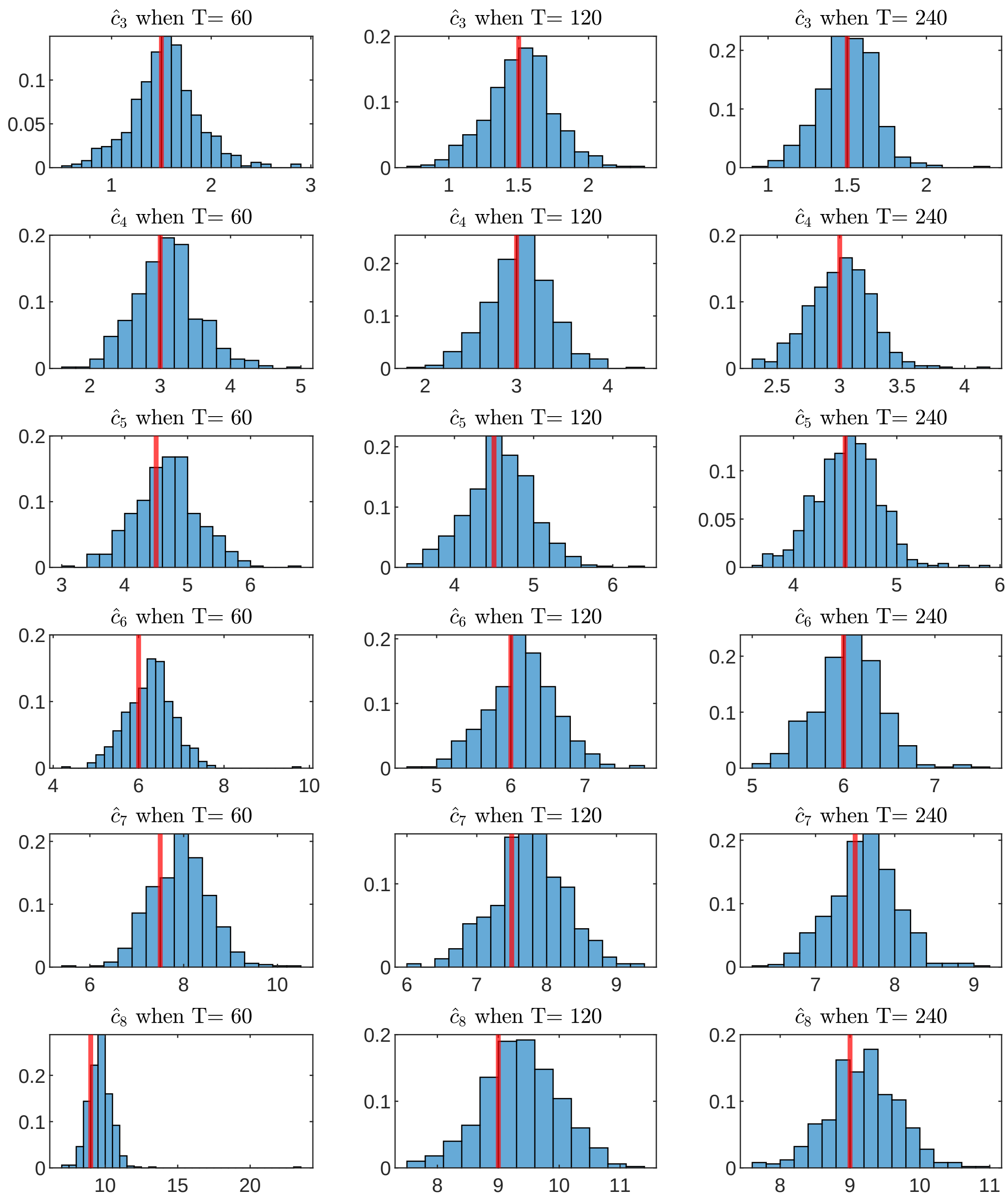

Figure 33: Empirical PDF for $\hat{\delta}_j$ when $\rho = 0$

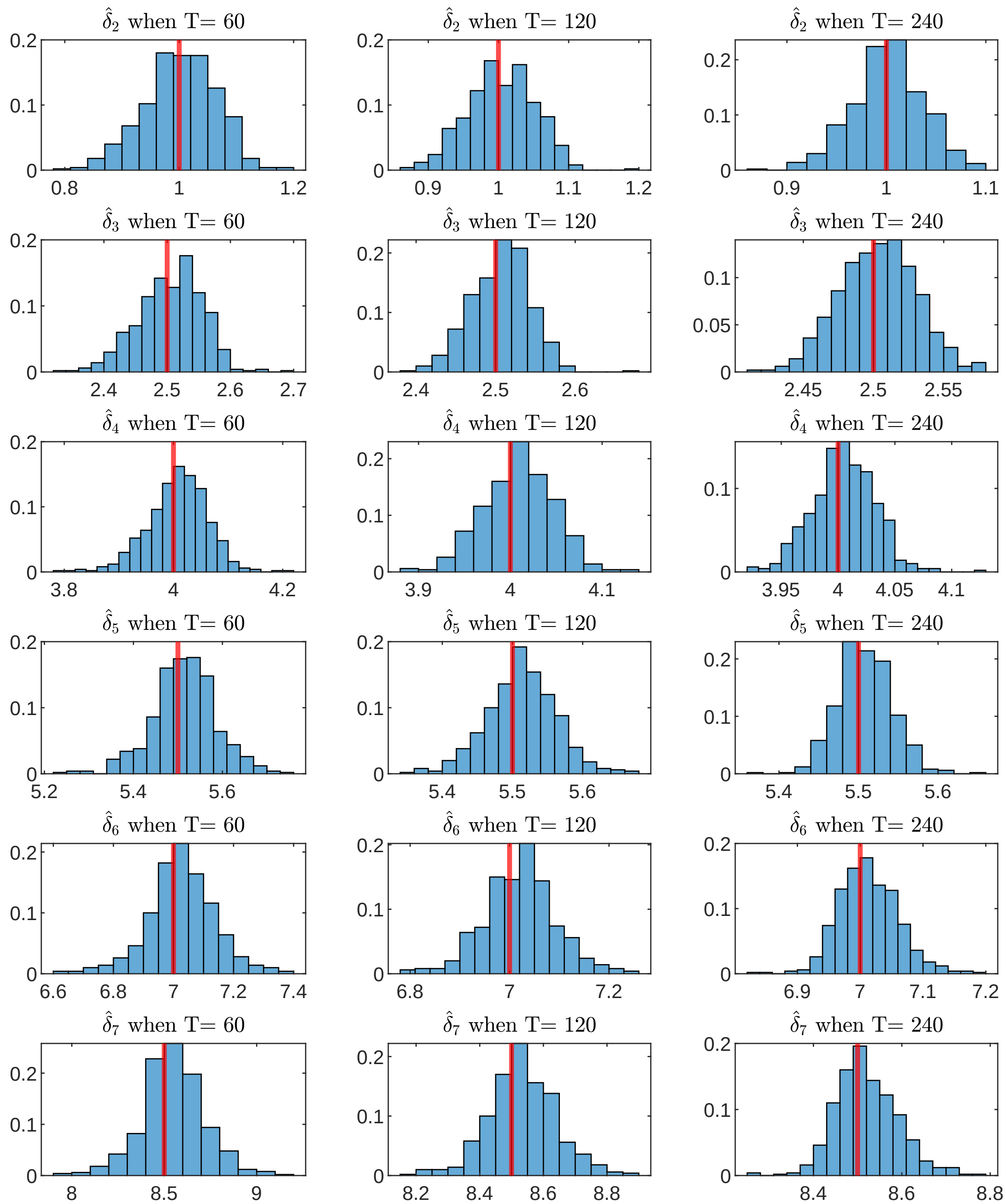

Figure 34: Empirical PDF for $\hat{\delta}_j$ when $\rho = 0.4$

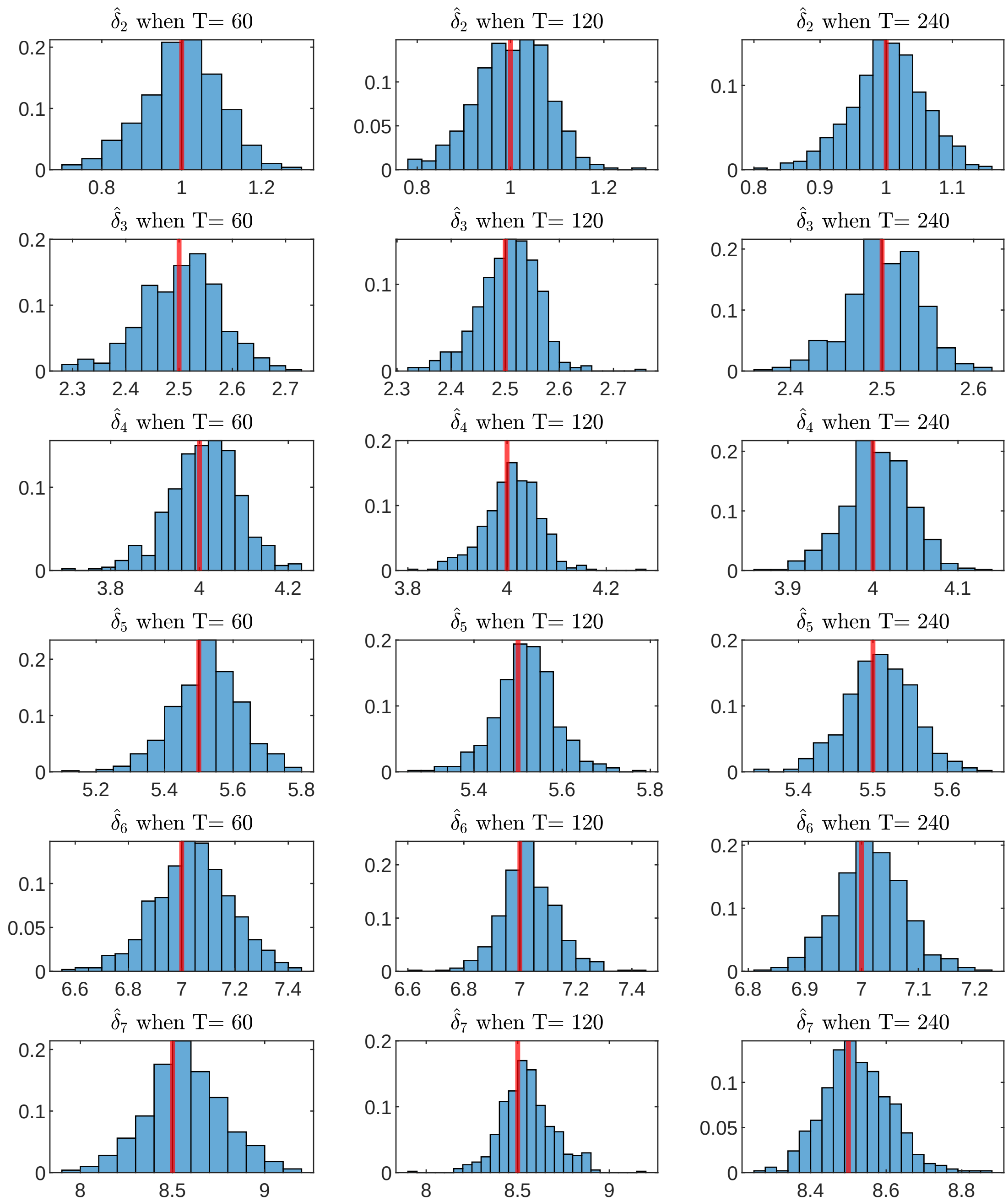

Figure 35: Empirical PDF for $\hat{\delta}_j$ when $\rho = 0.7$

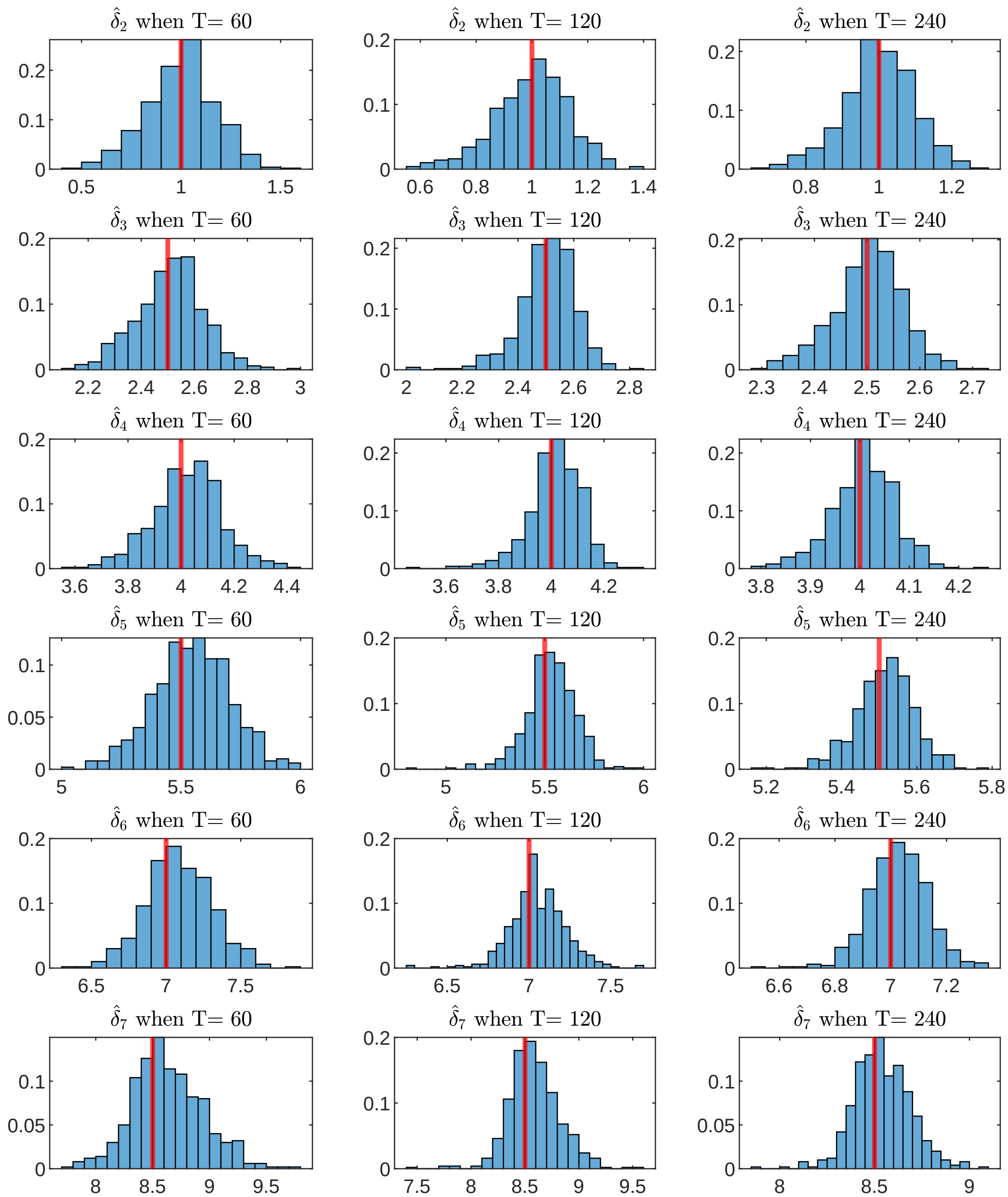

Figure 36: Empirical PDF for $\hat{\delta}_j$ when $\rho = 0.95$

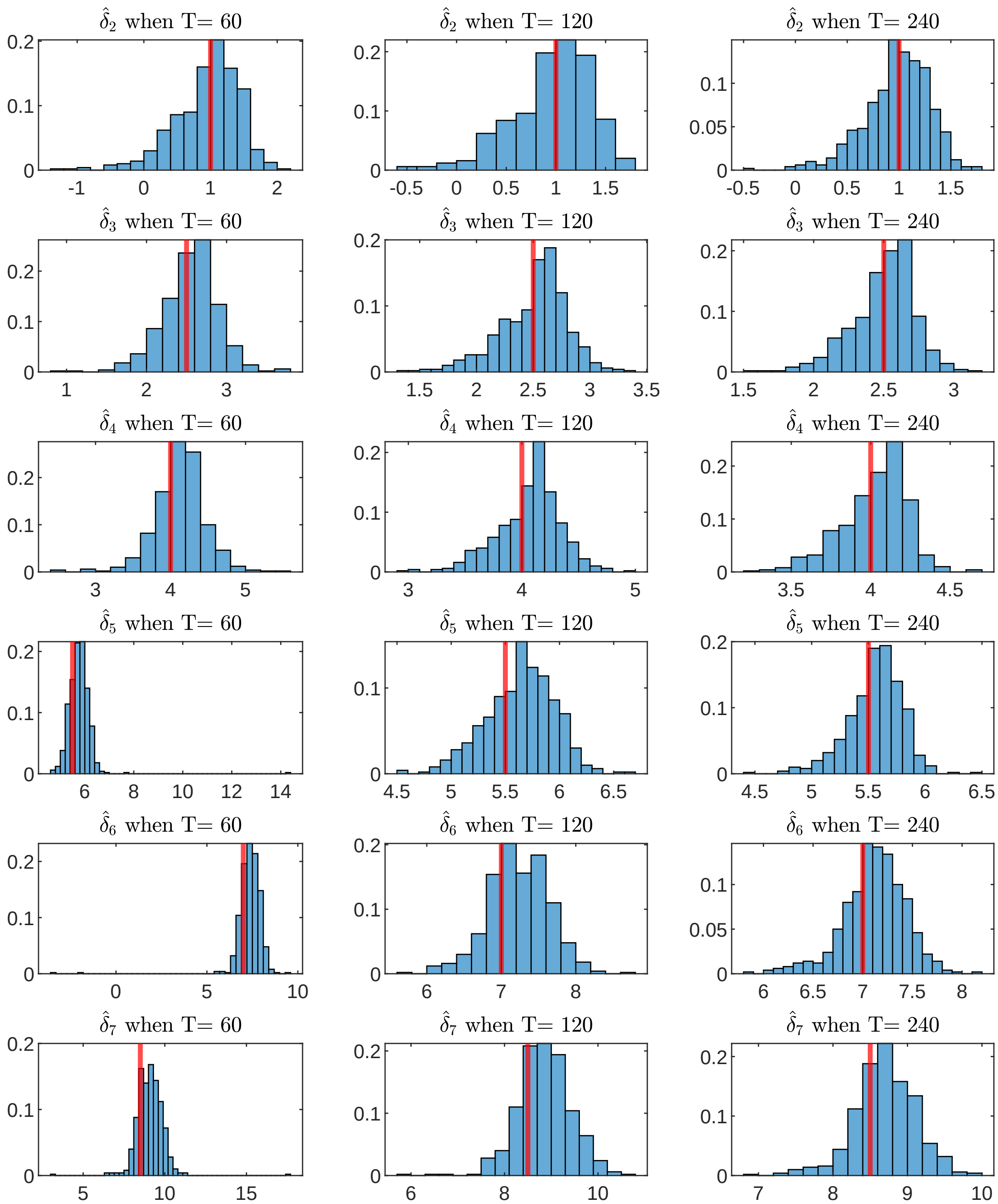

Figure 37: Empirical PDF for $\hat{\beta}_j$ when $\rho = 0$

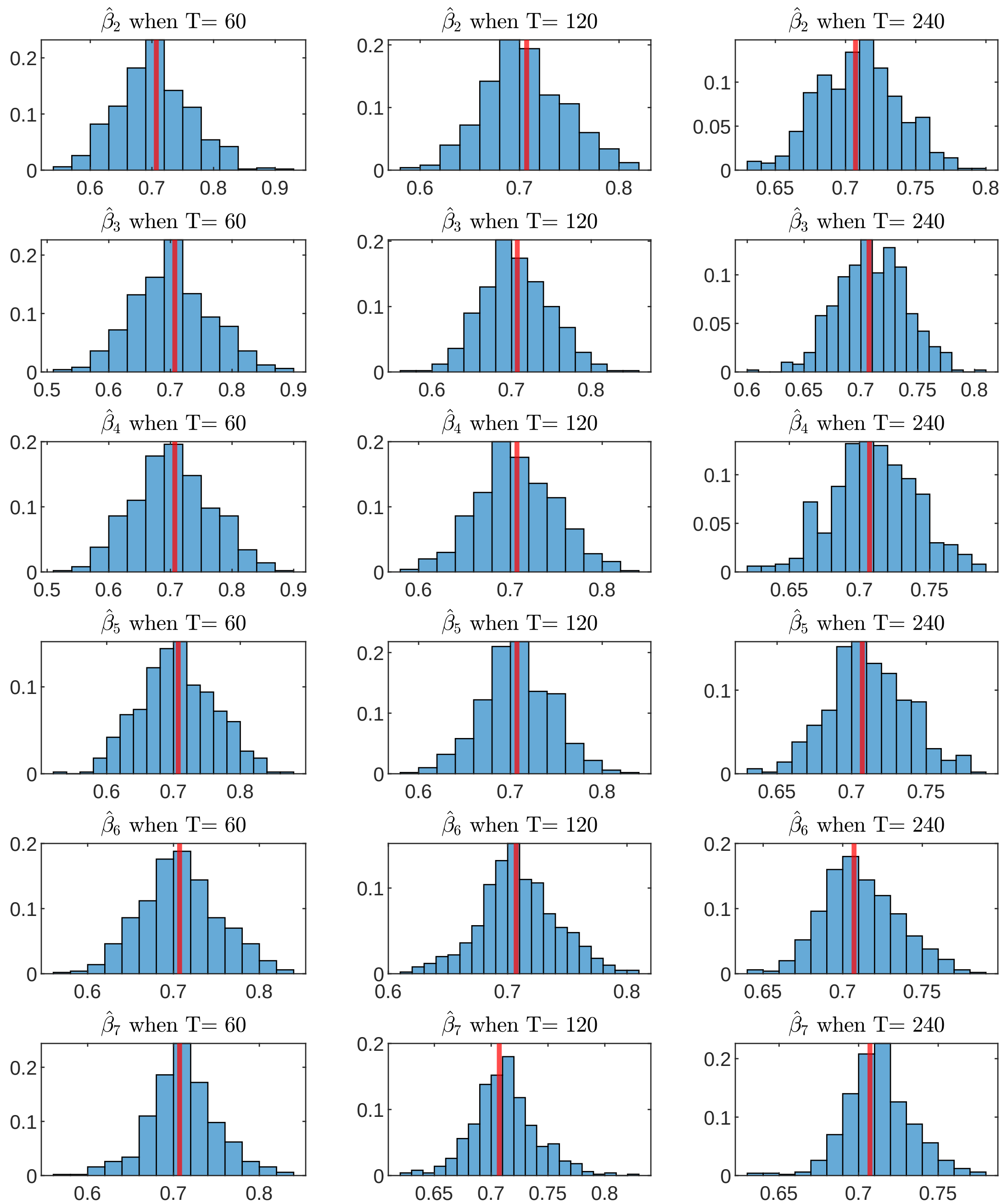

Figure 38: Empirical PDF of β_j when $\rho = 0.4$

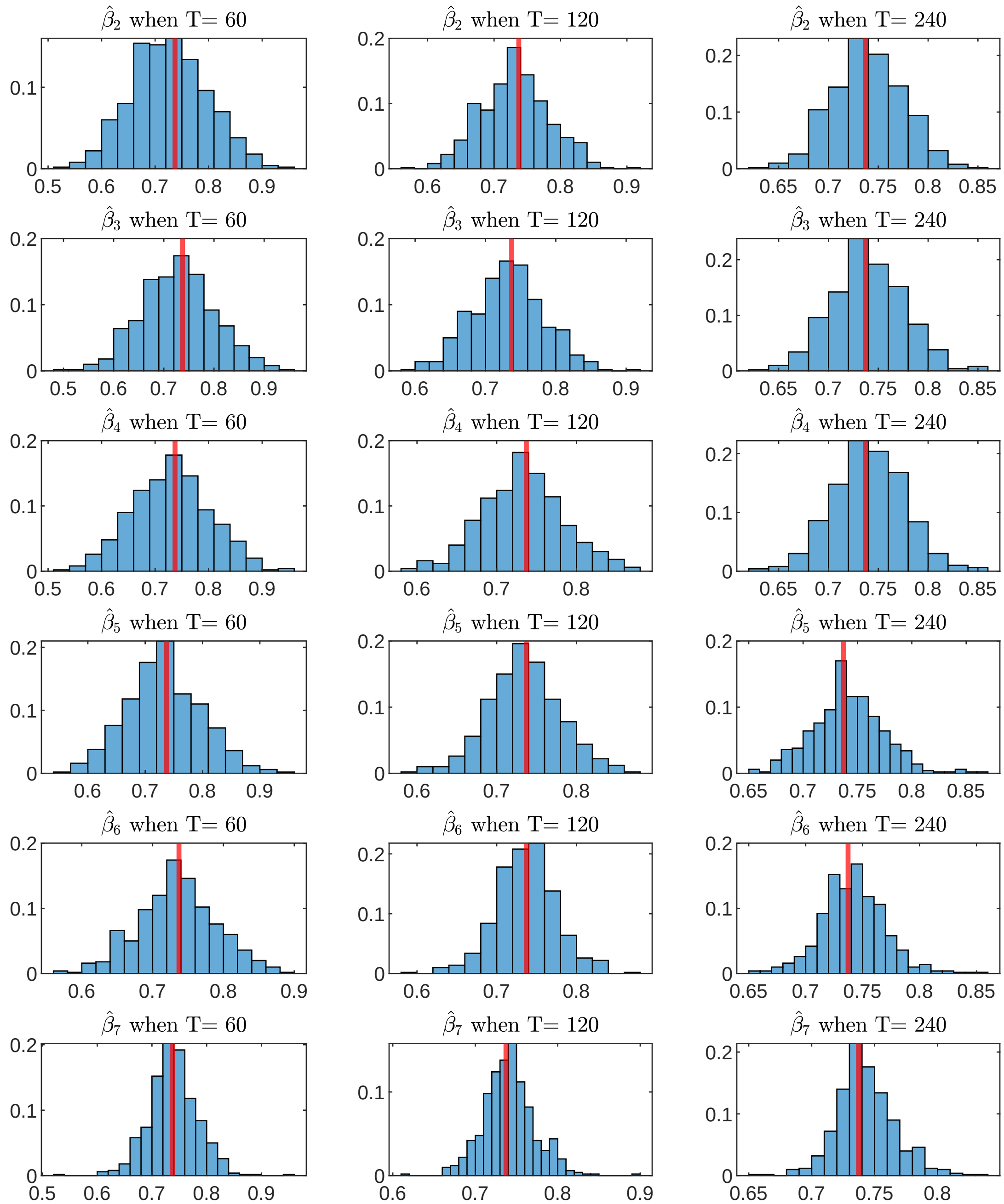

Figure 39: Empirical PDF for $\hat{\beta}_j$ when $\rho = 0.7$

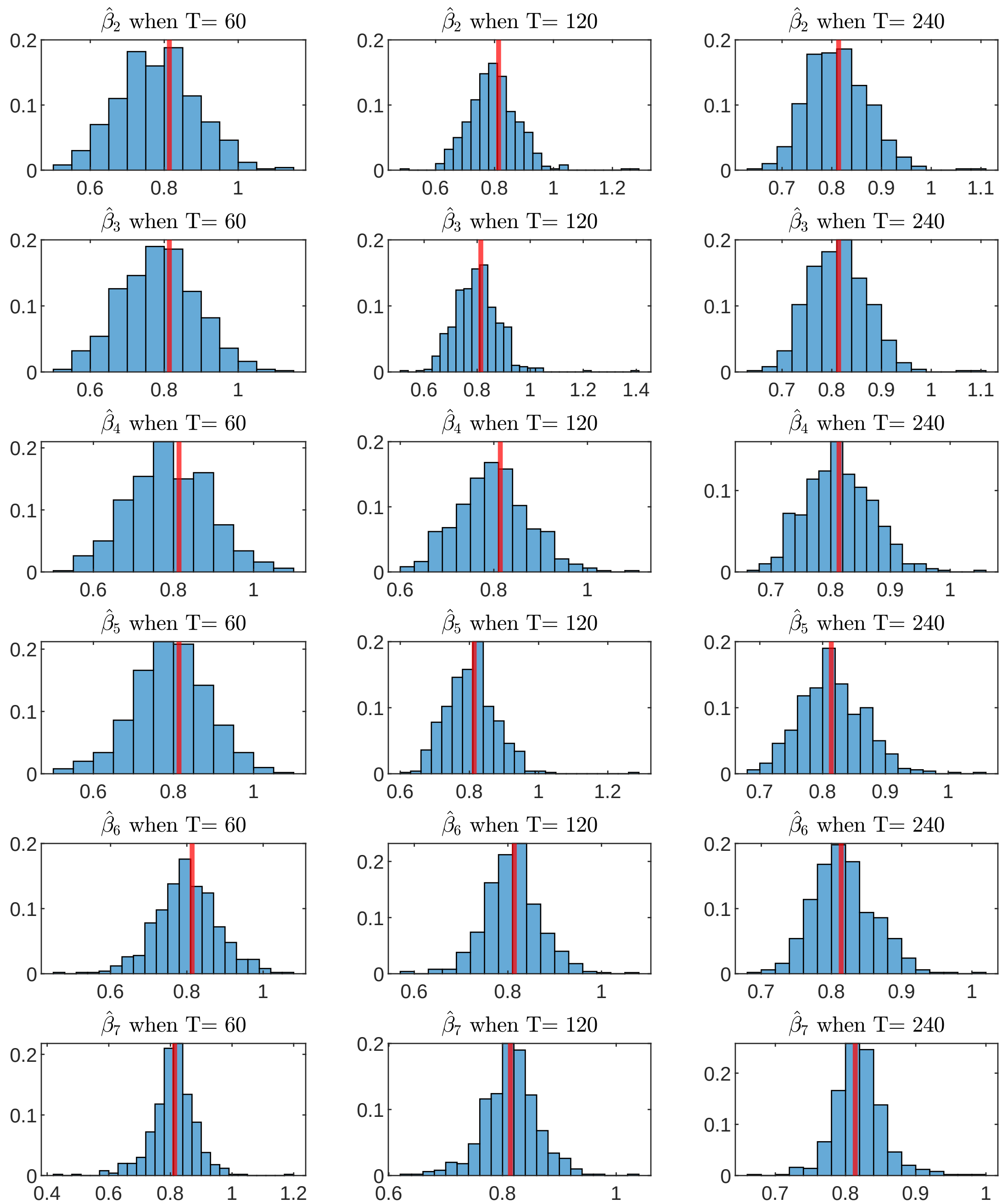

Figure 40: Empirical PDF of β_j when $\rho = 0.95$

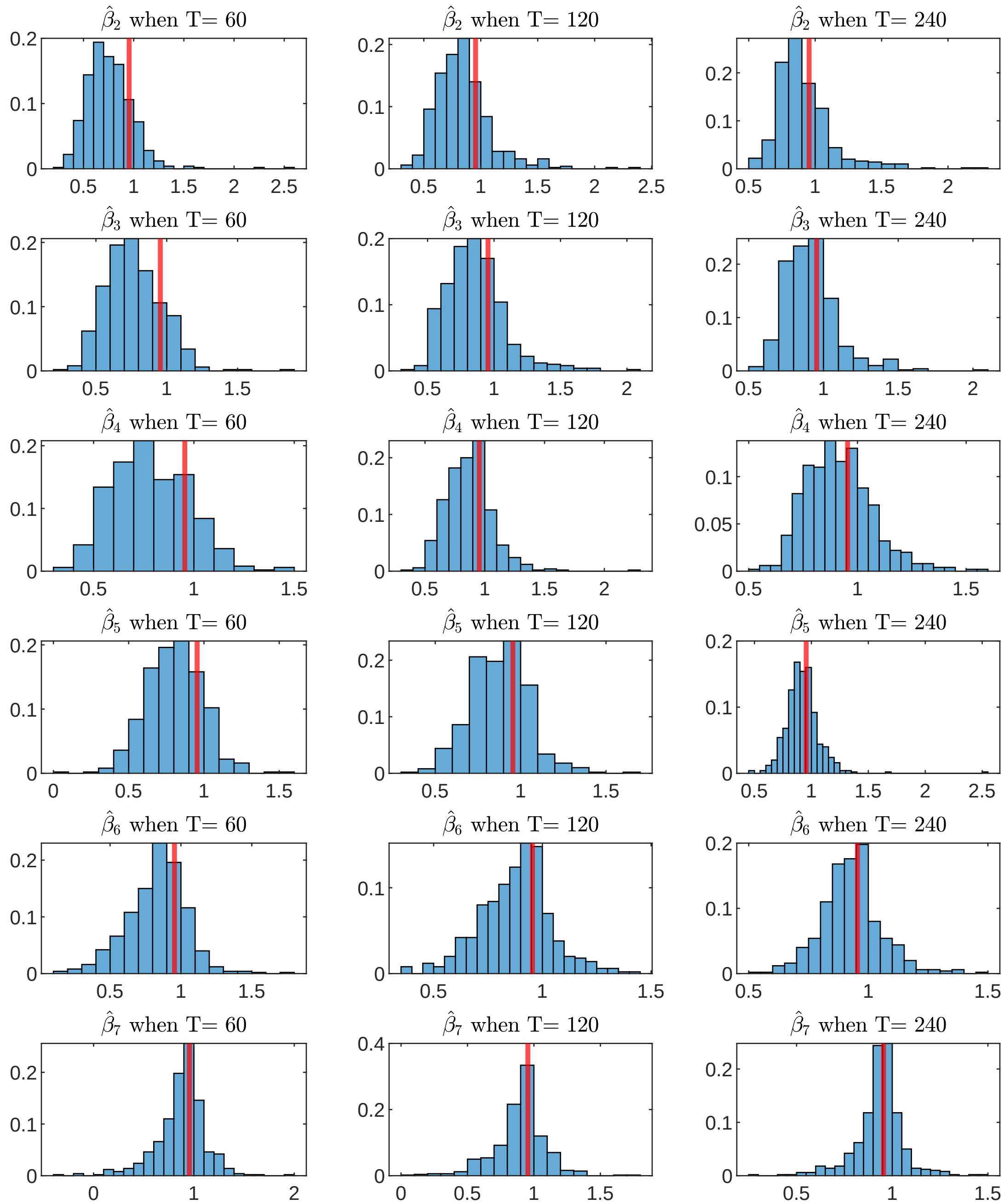

Figure 41: Empirical PDF for $\hat{\sigma}_j$ when $\rho = 0$

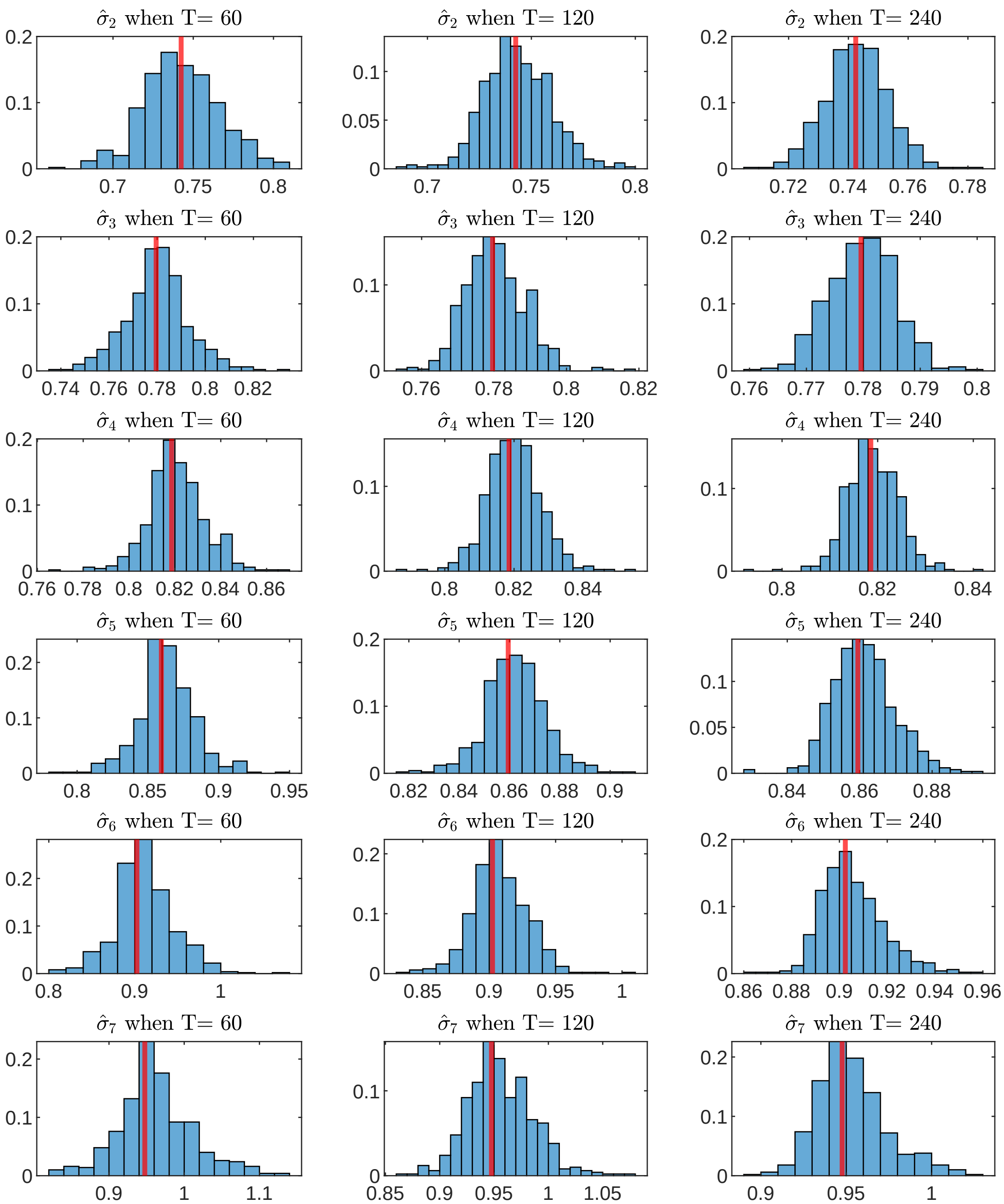

Figure 42: Empirical PDF for $\hat{\sigma}_j$ when $\rho = 0.4$

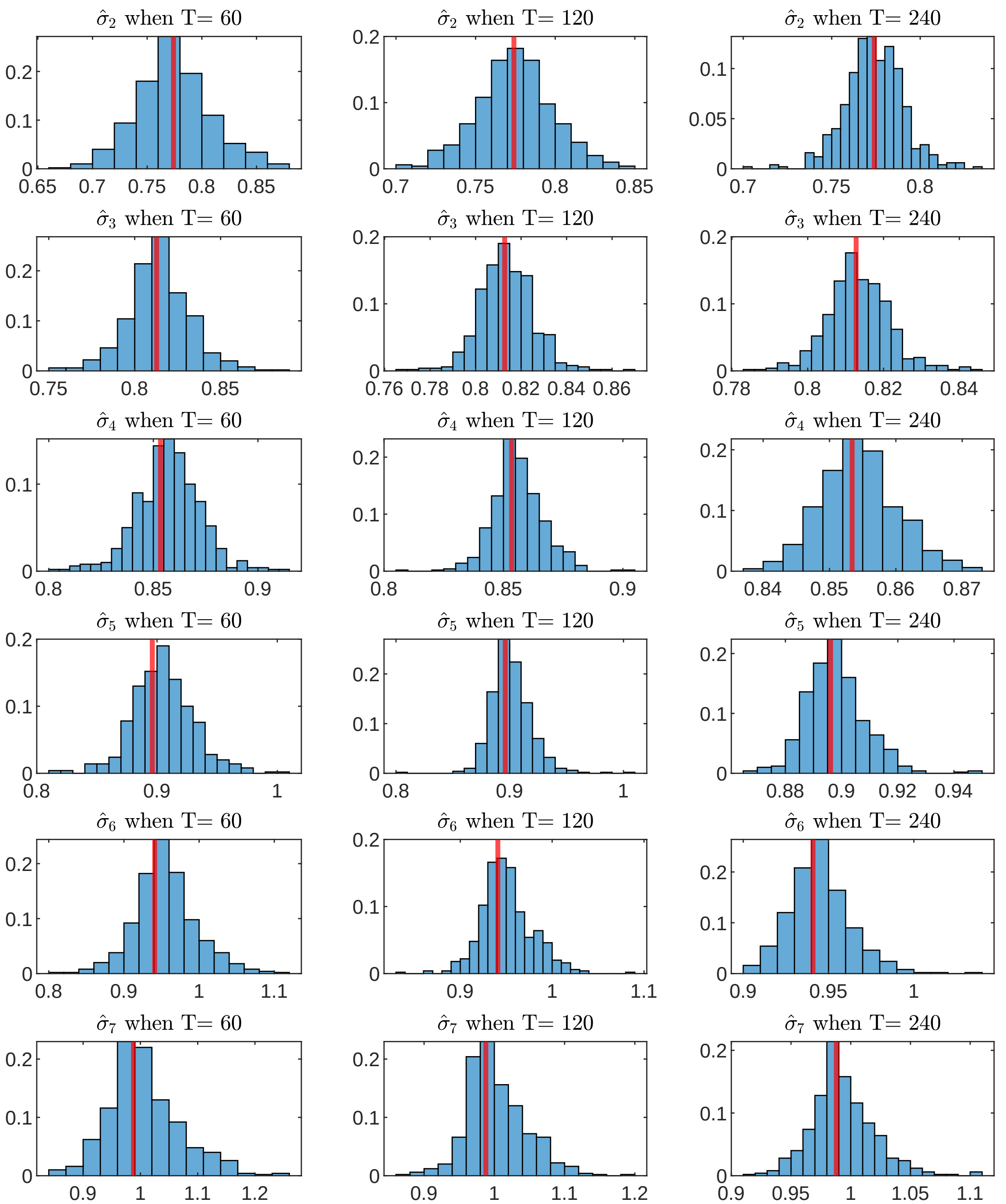

Figure 43: Empirical PDF for $\hat{\sigma}_j$ when $\rho = 0.7$

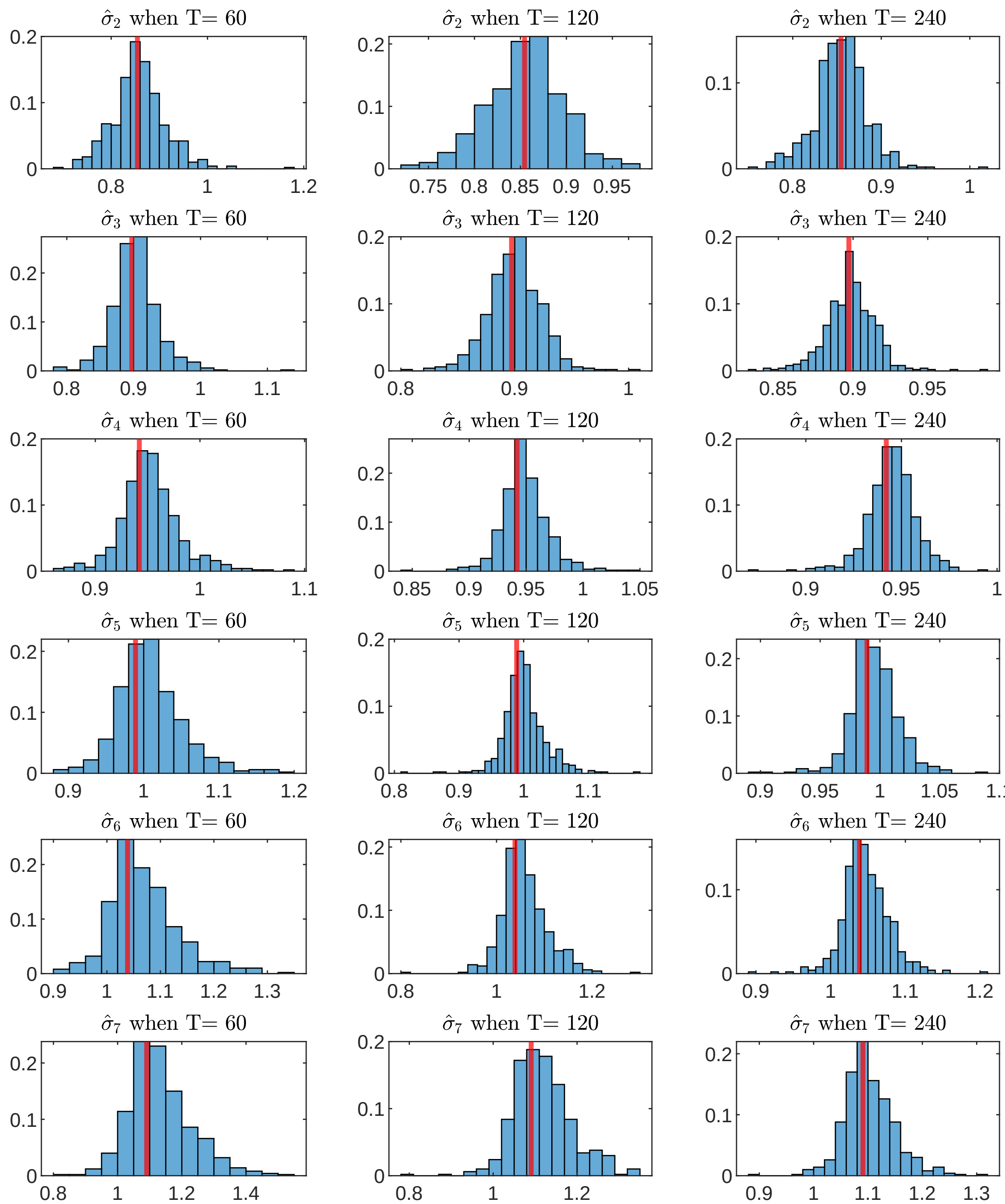

Figure 44: Empirical PDF for $\hat{\sigma}_j$ when $\rho = 0.95$

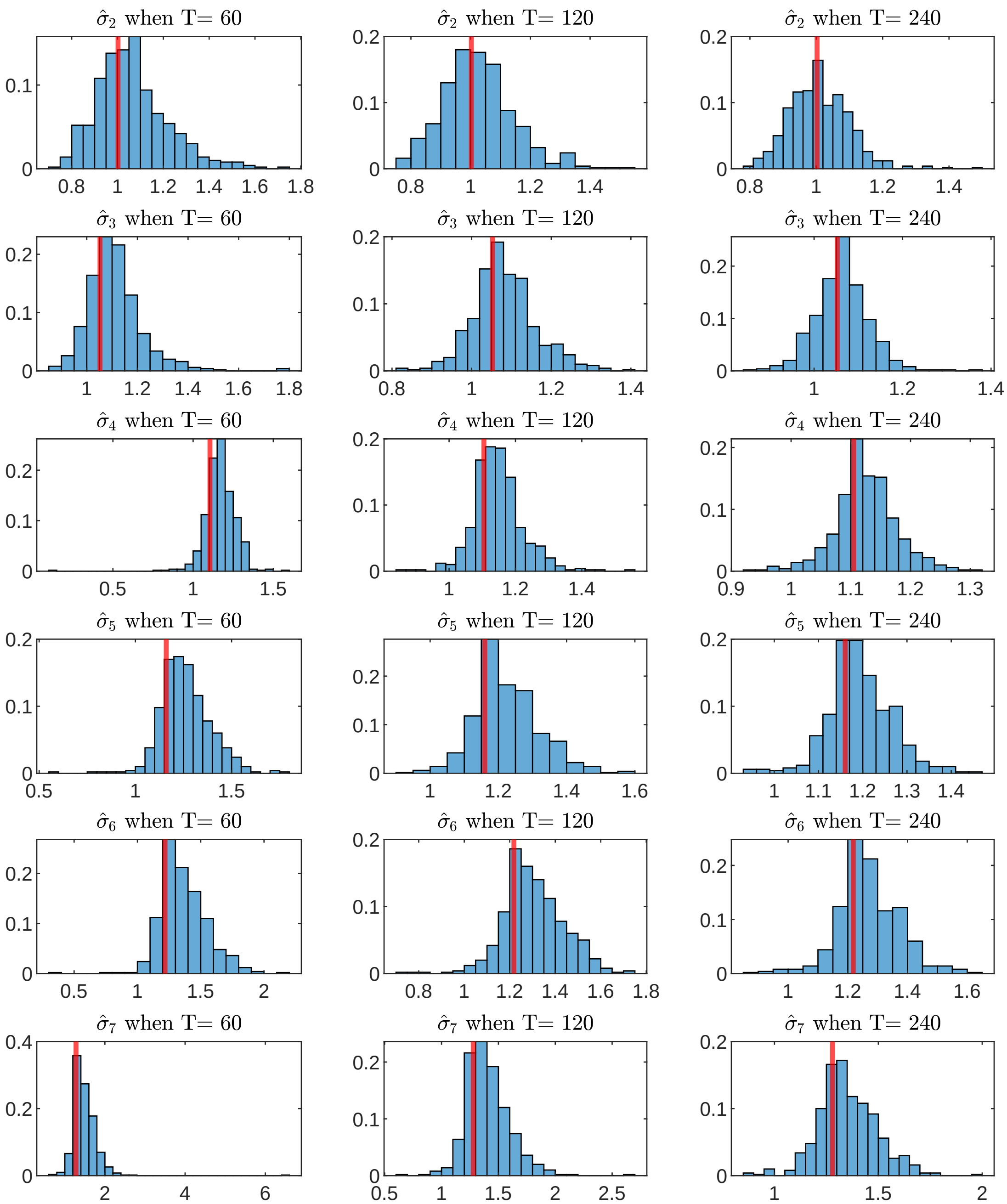

D.4. Figures for Average Simulated Rating Structures

Figure 45: Average Simulated Rating Structures when $\rho = 0$ and $T = 60$

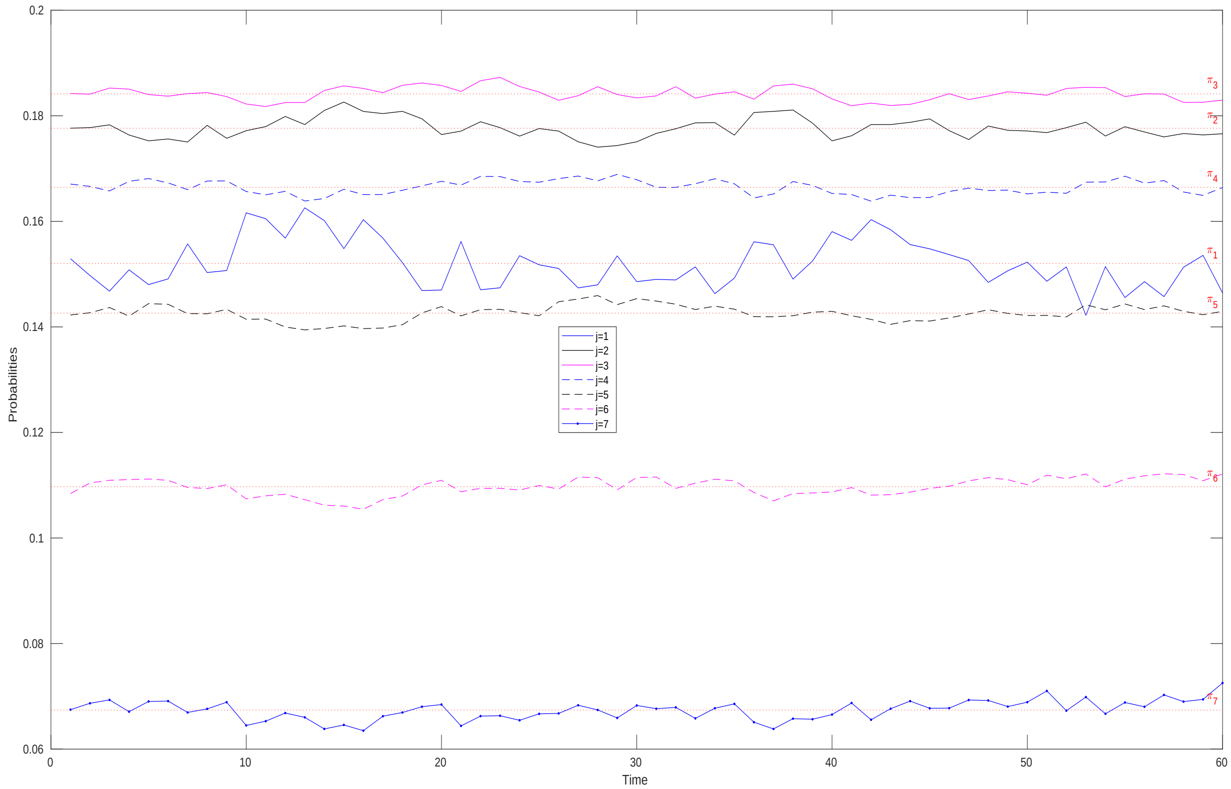

Figure 46: Average Simulated Rating Structures when $\rho = 0.4$ and $T = 60$

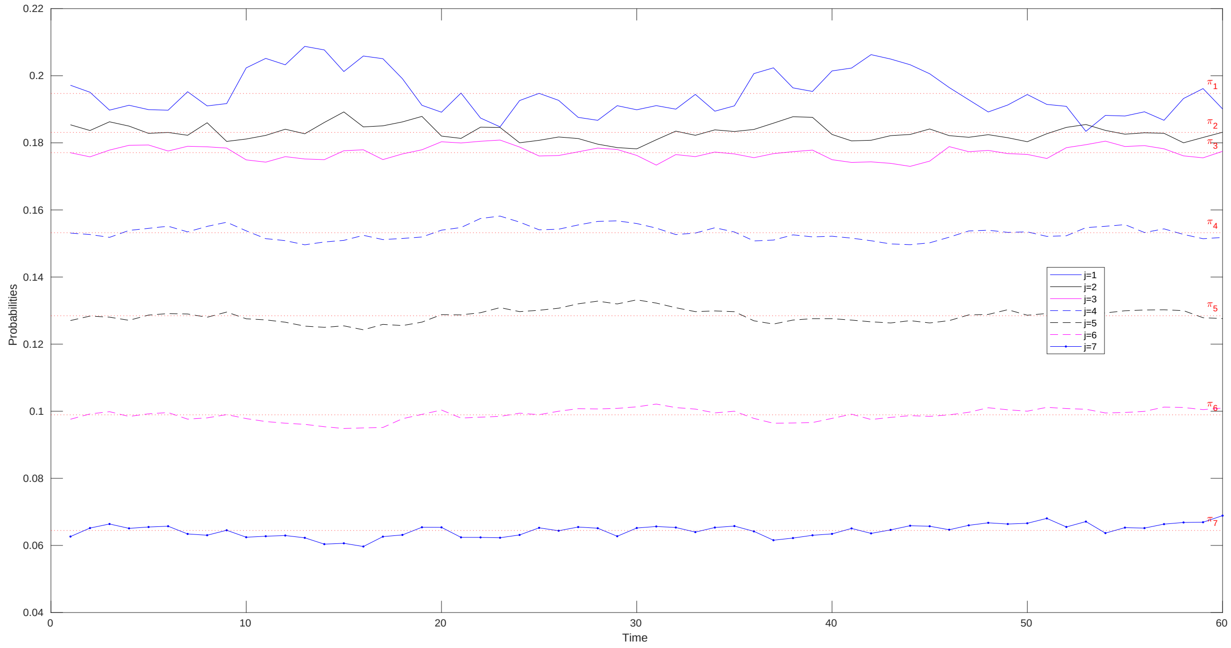

Figure 47: Average Simulated Rating Structures when $\rho = 0.7$ and $T = 60$

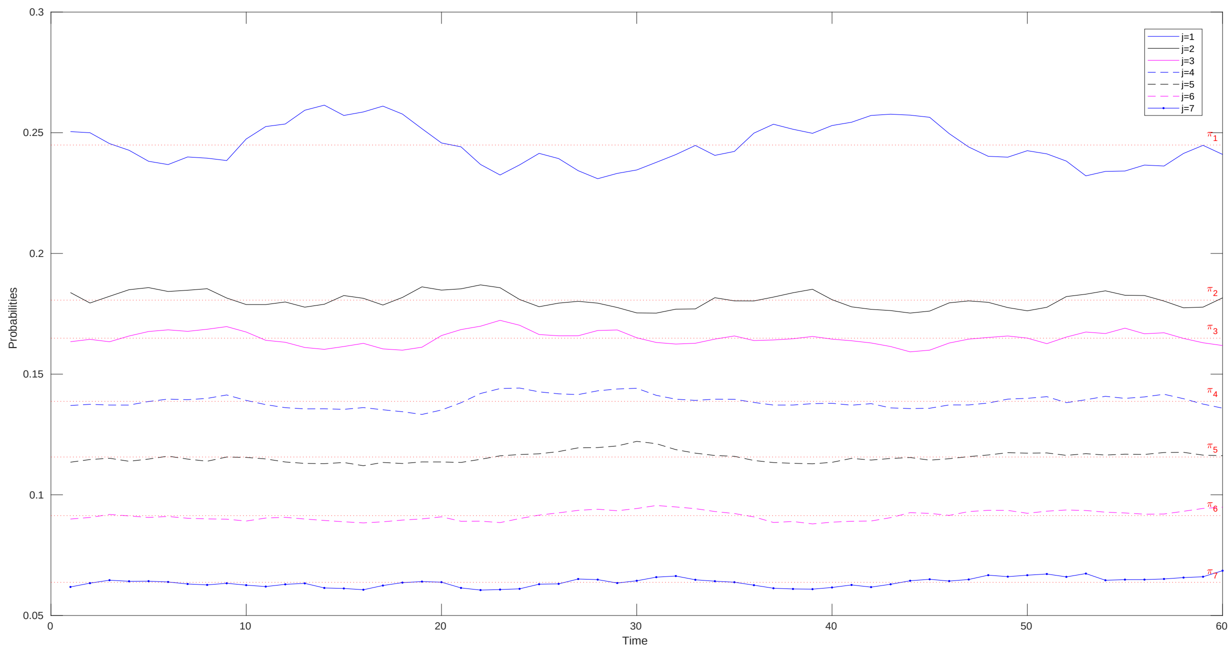

Figure 48: Average Simulated Rating Structures when $\rho = 0.95$ and $T = 60$

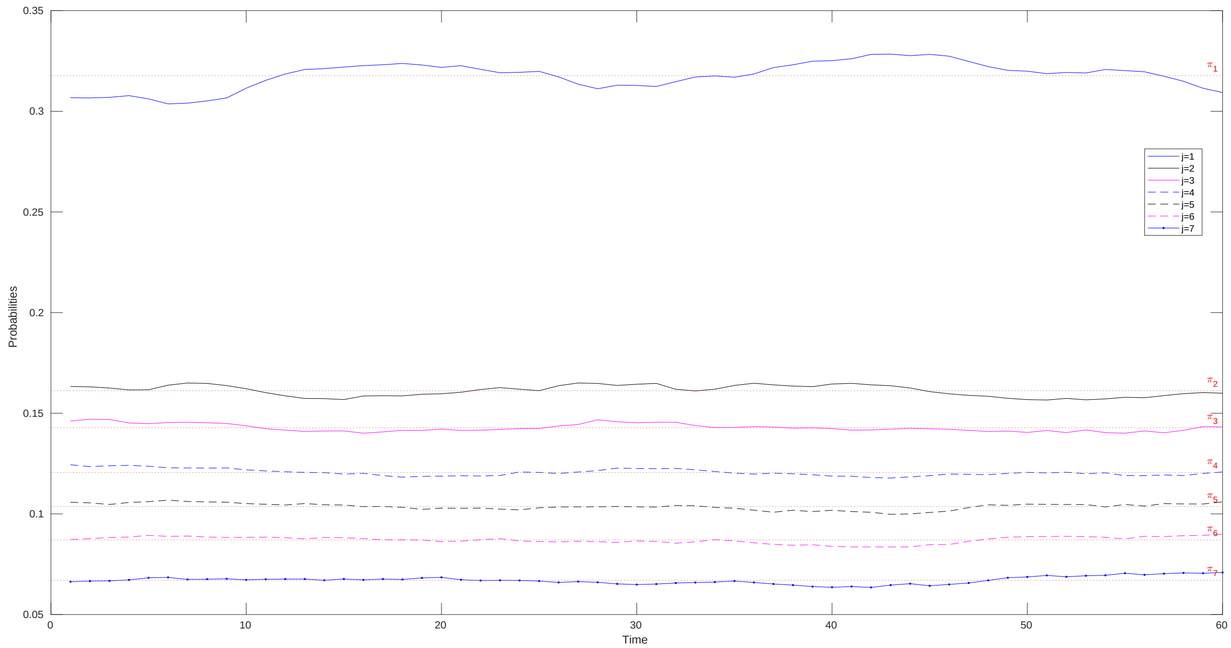

Figure 49: Average Simulated Rating Structures when $\rho = 0$ and $T = 120$

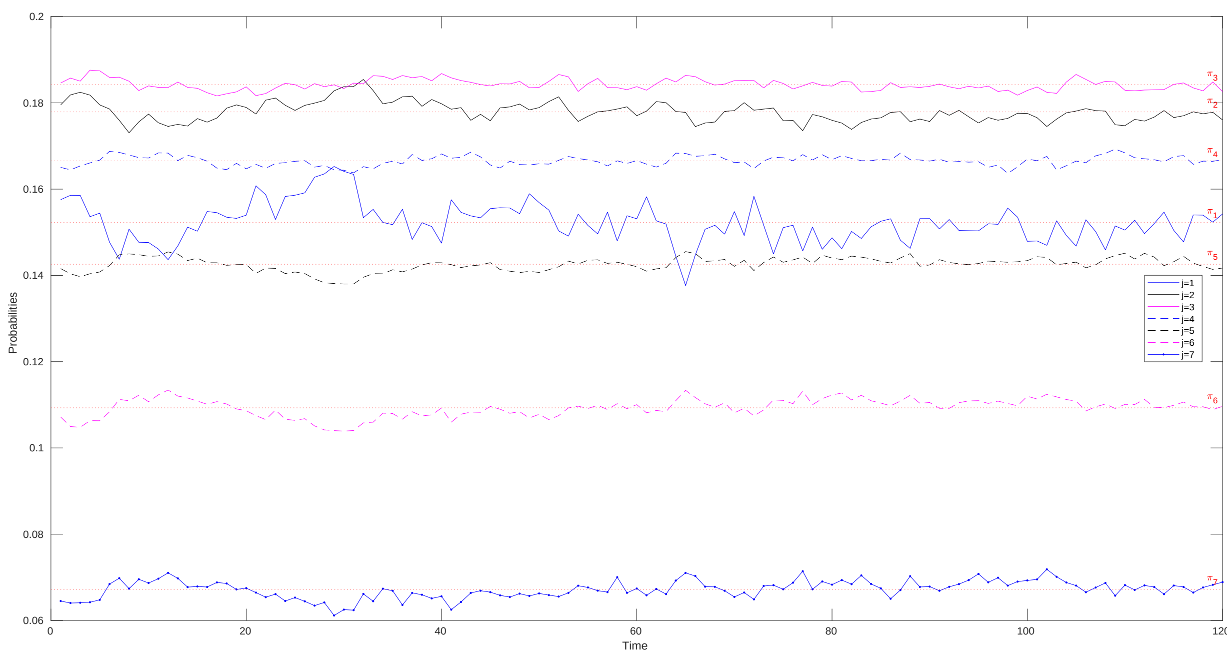

Figure 50: Average Simulated Rating Structures when $\rho = 0.4$ and $T = 120$

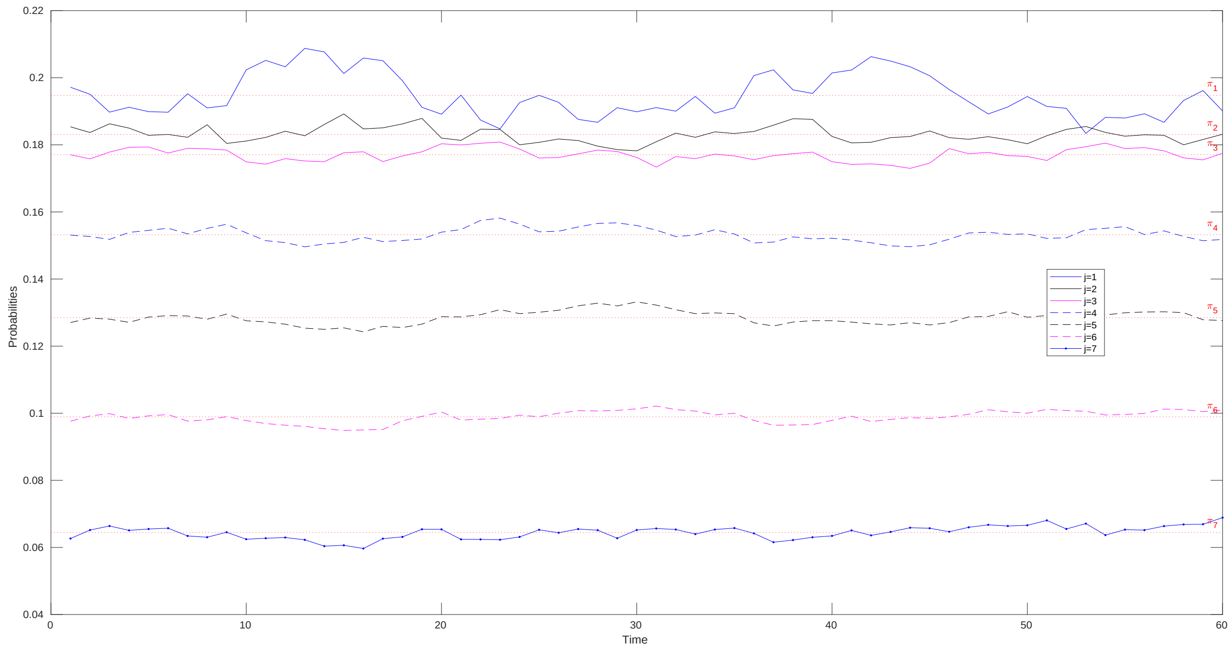

Figure 51: Average Simulated Rating Structures when $\rho = 0.7$ and $T = 120$

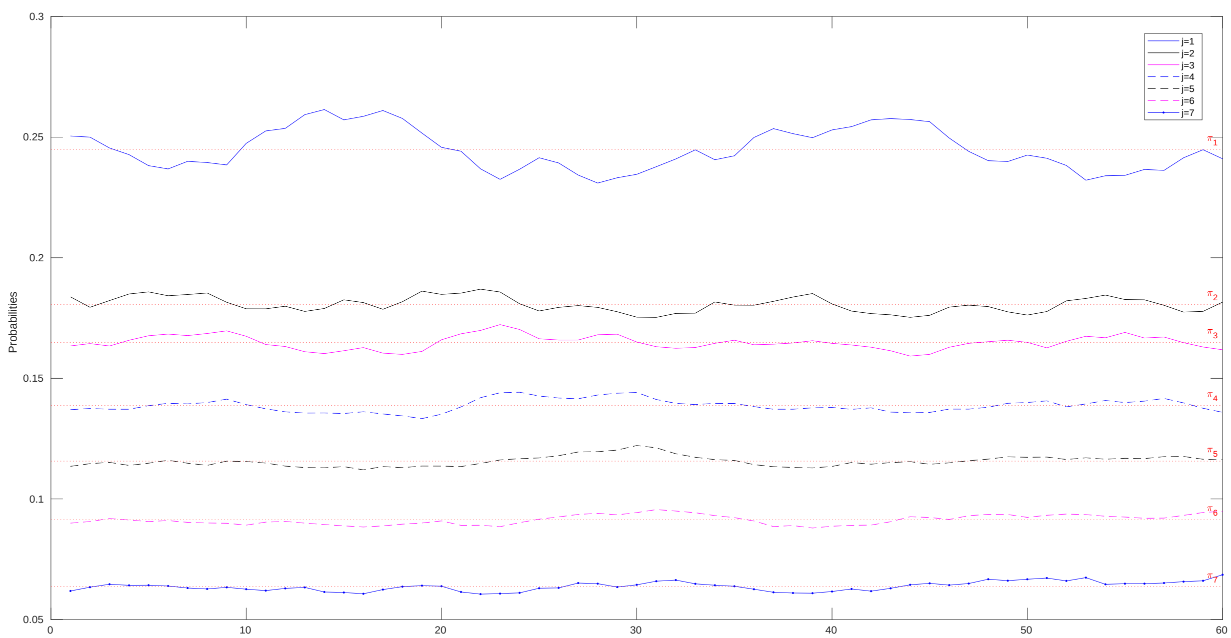

Figure 52: Average Simulated Rating Structures when $\rho = 0.95$ and $T = 120$

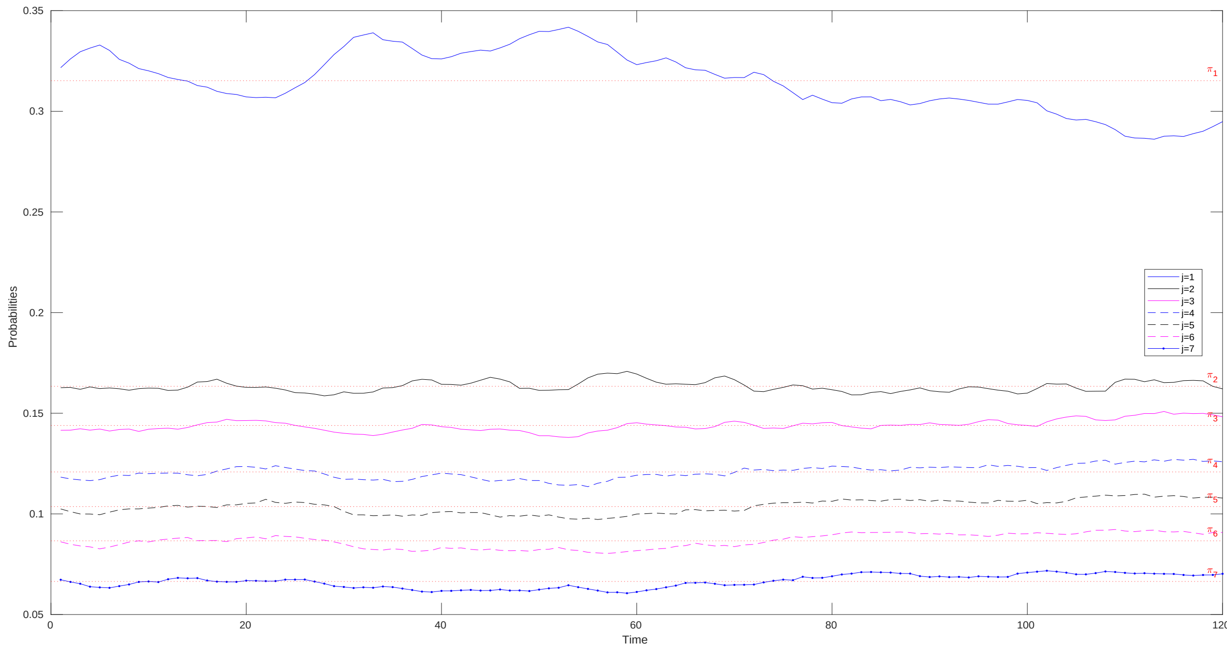

Figure 53: Average Simulated Rating Structures when $\rho = 0$ and $T = 240$

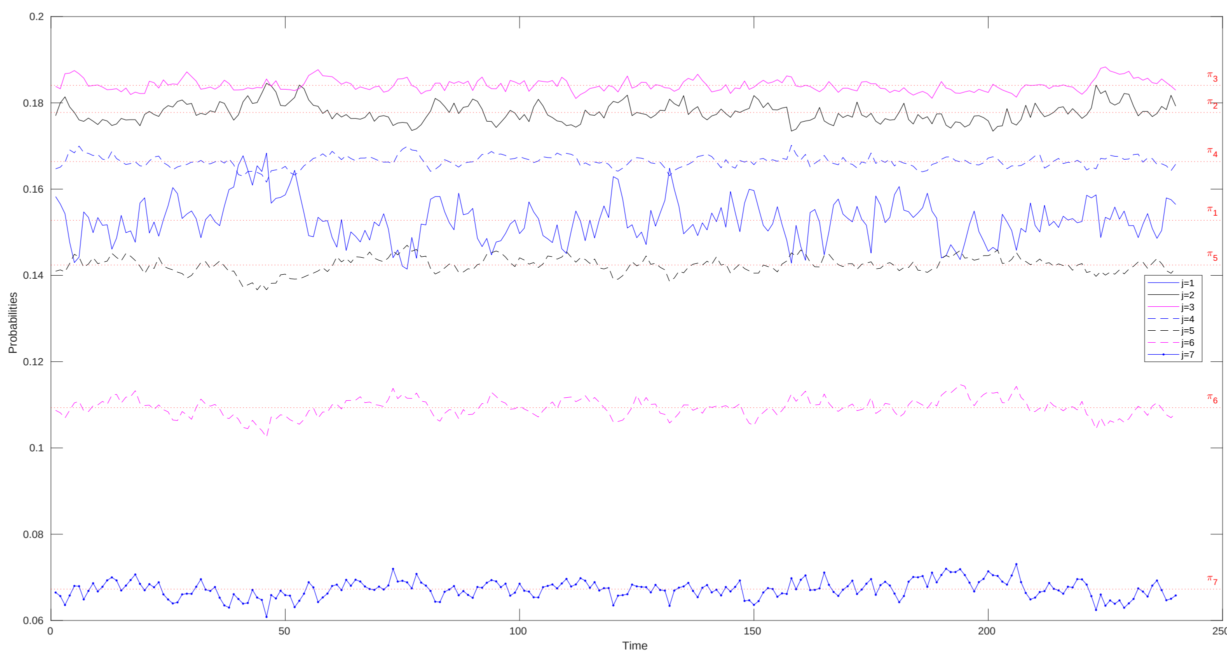

Figure 54: Average Simulated Rating Structures when $\rho = 0.4$ and $T = 240$

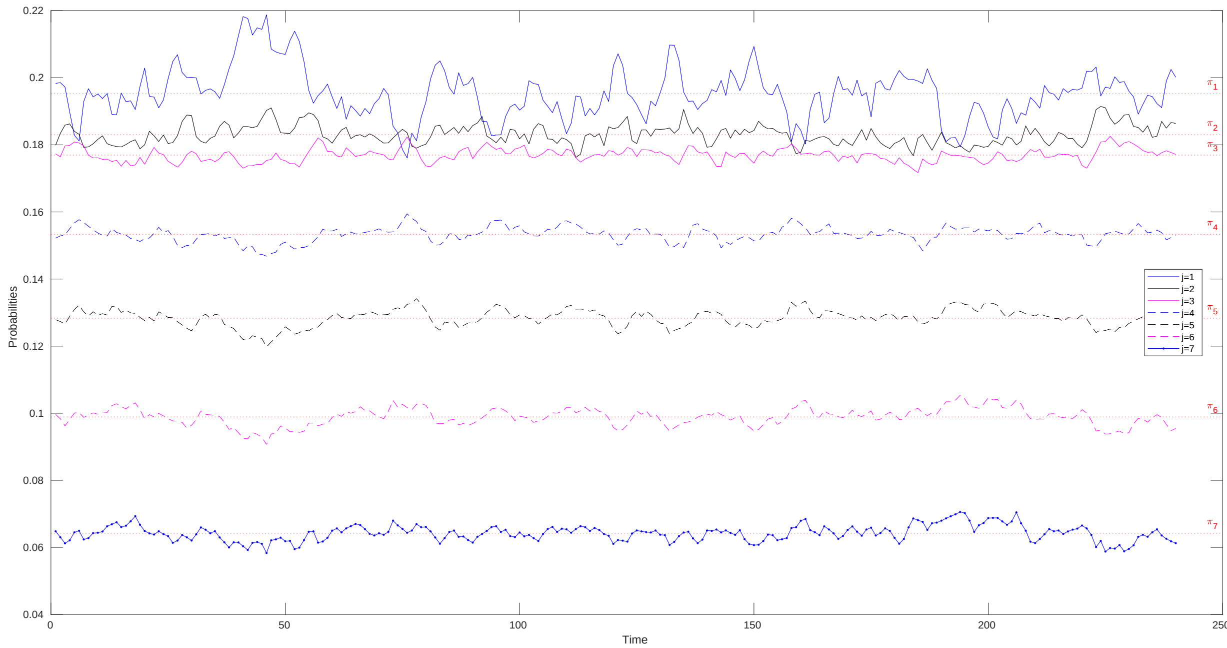

Figure 55: Average Simulated Rating Structures when $\rho = 0.7$ and $T = 240$

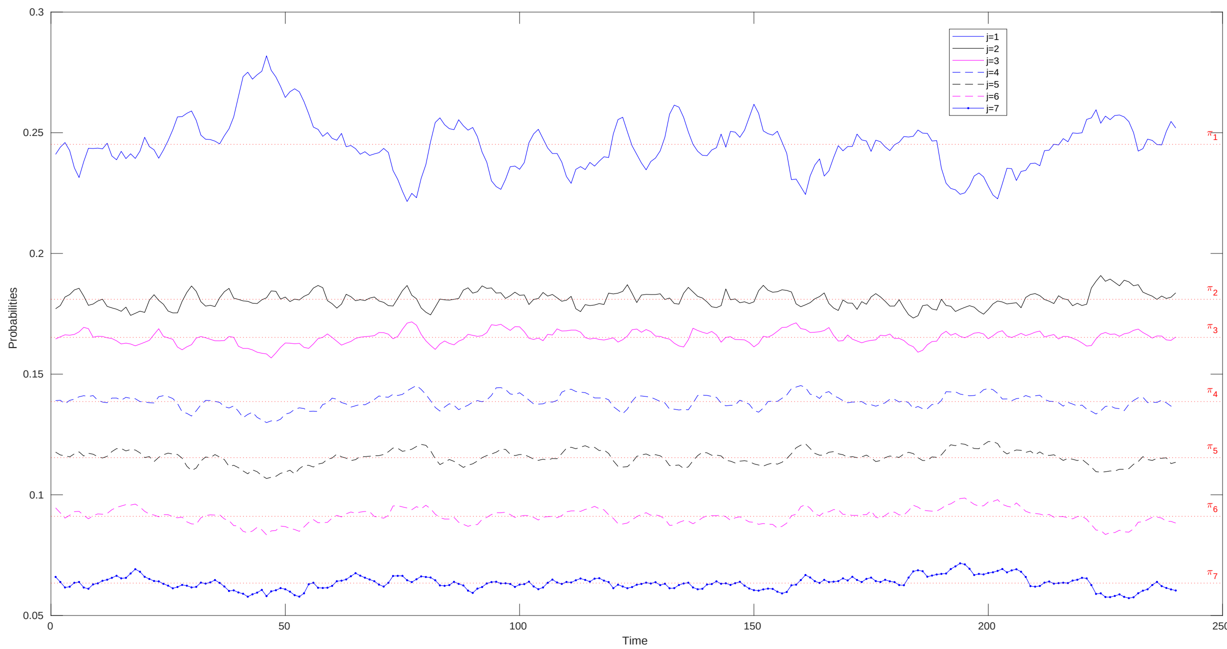

Figure 56: Average Simulated Rating Structures when $\rho = 0.95$ and $T = 240$